AAEC/E517

AAEC/E517

AUSTRALIAN ATOMIC ENERGY COMMISSION

RESEARCH ESTABLISHMENT

LUCAS HEIGHTS

AN INVESTIGATION OF CRITICAL HEAT FLUXES IN VERTICAL TUBES INTERNALLY COOLED BY FREON-12 PART I - CRITICAL HEAT FLUX EXPERIMENTS WITH AXIALLY UNIFORM AND NON-UNIFORM HEATING AND COMPARISONS OF DATA WITH SELECTED CORRELATIONS

by

W.J. GREEN

J.R. STEVENS

August 1981

ISBN 0 642 59716 2

AUSTRALIAN ATOMIC ENERGY COMMISSION
RESEARCH ESTABLISHMENT
LUCAS HEIGHTS

AN INVESTIGATION OF CRITICAL HEAT FLUXES IN VERTICAL TUBES INTERNALLY COOLED BY FREON-12
PART I - CRITICAL HEAT FLUX EXPERIMENTS WITH AXIALLY UNIFORM AND NON-UNIFORM HEATING AND COMPARISONS OF DATA WITH SELECTED CORRELATIONS

by

W.J. GREEN
J.R. STEVENS

ABSTRACT

Experiments have been performed using vertical heated tubes, cooled internally by Freon-12, to determine critical heat fluxes (CHFs) for both a uniformly heated section and an exit region with a separately controlled power supply. Heated lengths of the main sections were 2870 mm (for 8.48 and 16.76 mm tube bores) and 3700 mm (for 21.34 mm tube bore); heated length of the exit section was 230 mm. Coolant pressures, exit qualities and mass fluxes were in the range 0.9 to 1.3 MPa, 0.19 to 0.86 and 380 to 2800 kg m^{-2} s^{-1}, respectively.

(Continued)

The data have been compared with published empirical correlations specifically formulated to predict CHFs in Freon-cooled, vertical tubes; relevant published CHF data have also been compared with these correlations. These comparisons show that, even over the ranges of conditions for which the correlations were developed, predicted values are only accurate to within ± 20 per cent. Moreover, as mass fluxes increase above 3500 kg m^{-2} s^{-1}, the modified Groeneveld correlation becomes increasingly inadequate, and the Bertoletti and modified Bertoletti correlations under-predict CHF values by increasing amounts. At mass fluxes below 750 kg m^{-2} s^{-1} the Bertoletti correlations exhibit increasing inaccuracy with a decrease in mass flux.

For non-uniform heating, the correlations are at variance with the experimental data, indicating, as was found by others, that the inherent assumptions of thermal equilibrium and average local coolant conditions are inadequate. The results show that under these conditions, local CHF values can be substantially less than would be predicted from correlations of this type.

National Library of Australia card number and ISBN 0 642 59716 2

The following descriptors have been selected from the INIS Thesaurus to describe the subject content of this report for information retrieval purposes. For further details please refer to IAEA-INIS-12 (INIS: Manual for Indexing) and IAEA-INIS-13 (INIS: Thesaurus) published in Vienna by the International Atomic Energy Agency.

CRITICAL HEAT FLUX; HEAT TRANSFER; DRYOUT; BURNOUT; TUBES; ORGANIC COOLANTS; REACTOR COOLING SYSTEMS; FREONS; FLUID FLOW; TRANSIENTS

CONTENTS

(Continued)

CONTENTS (Continued)

CONTENTS (Continued)

1. INTRODUCTION

Over the last two decades there have been many experimental [Bertoletti et al. 1964; Stevens et al. 1964; Groeneveld 1969; Merilo and Ahmad 1979] and semi-theoretical [Shah 1978; Katto 1978] investigations aimed at understanding, correlating and predicting the onset of dryout (or the critical heat flux) in a round tube.

In recent experiments at the AAEC's Research Establishment, the heat transfer characteristics associated with a change from pre-dryout to post-dryout conditions during a power transient [Green 1978; Green and Lawther 1979; Green and Lawther 1980] have been investigated with particular emphasis on the post-dryout regimes. These investigations used a vertical round tube test section, electrically heated and cooled internally by Freon-12 flowing at relatively low mass fluxes. Heat transfer characteristics were determined by calculating wall temperature responses as a function of time and comparing these with the corresponding temperature traces in the experiments. The comparisons showed that the calculated temperature responses were very sensitive to the prediction of the onset of dryout. It was found that the Bertoletti [1964] and Groeneveld [1969] correlations were not accurate in predicting critical heat fluxes for tubes with either uniform or non-uniform heating.

Modified correlations were developed by Green [1978] for a uniformly heated tube, but were found to be unsuitable by Green and Lawther [1980] when used on a local conditions basis for tubes heated non-uniformly. It was therefore considered that further steady-state CHF data should be obtained from a wide range of mass fluxes (300 to 3000 kg m^{-2} s^{-1}), for both uniformly and non-uniformly heated test sections, to determine whether the available correlations could be modified to make them predict more accurately the onset of dryout for these flow conditions. Three sizes of tube, heated in two sections, were used. Initial data indicated that predicted values using the original and modified versions of Bertoletti and Groeneveld correlations had a tendency to become more inaccurate at larger mass fluxes.

To examine the validity of this observation, published steady state experimental CHF data for Freon-12 in uniformly heated round tubes were compared with predictions of the Bertoletti and Groeneveld correlations and their modified versions. To indicate the manner in which the project developed and broadened its objectives, the analysis of published experimental

data is discussed after the experimental work.

2. CRITICAL HEAT FLUX CORRELATIONS DEVELOPED FOR FREON-12 IN UNIFORMLY HEATED ROUND TUBES

Many empirical correlations [Barnett 1963; Thompson and Macbeth 1964; Biasi et al. 1967; Bowring 1972; Roko et al. 1978] have been developed to predict critical heat fluxes in heated tubes cooled by water. However, including those of Groeneveld [1969] and Bertoletti et al. [1964], only a few correlations have been formulated for systems having round tubes cooled internally by Freon-12.

2.1 Groeneveld Correlation

The Groeneveld correlation was developed specifically to represent experimental CHF data obtained on the Freon-12 heat transfer facility operated at Chalk River by Atomic Energy of Canada Ltd (AECL).

Assuming that the CHF could be related to the tube bore, heated length, mass flux and inlet enthalpy, the experimental data were used to express empirically the effects of tube bore, ratio of heated length to tube bore, mass flux and coolant quality at the point of burnout as polynomial functions having the form

$$PHIG = D^{b}\, f(L/D)\, f(G)\, f(X)$$

where, as expressed by Groeneveld in British Imperial units,

$$b = -0.362713$$

$$f(L/D) = 9.71043 \times 10^{6} - 2.17140 \times 10^{4}\,(L/D) + 42.2492\,(L/D)^{2}$$

$$f(G) = 1.16244 \times 10^{-2} - 1.150610 \times 10^{-2}\,(G/10^{6}) + 6.28448 \times 10^{-3}\,(G/10^{6})^{2} - 1.17288 \times 10^{-3}\,(G/10^{6})^{3}$$

$$f(X) = 1.36368 - 2.88422X + 3.52880X^2 - 2.23072X^3$$

There are some obvious deficiencies in this type of correlation, i.e.

- negative values of critical heat flux are predicted at exit qualities above 0.9;
- above an L/D ratio of 257, the critical heat flux is predicted to increase with increasing L/D values; and
- for mass fluxes greater than approximately 4400 kg m^{-2} s^{-1}, critical heat fluxes will have negative values.

The first two anomalies were eliminated by modifying the correlation [Green 1978] so that when X was greater than 0.6:

$$f(X) = 0.724012 - 0.5042012X$$

and, for L/D greater than 200,

$$f(L/D) = [7.762663 - 0.00352533\ (L/D)]\ 10^6 \quad .$$

In the following comparisons between experimental data and predicted values, the modified version of the Groeneveld correlation has been used.

2.2 The Bertoletti Correlation

Often termed the CISE correlation, this correlation was developed to represent CHF data obtained for water. Bertoletti found, however, that by merely changing an empirical numerical factor, the correlation could also represent Freon-12 data.

Unlike the Groeneveld correlation, the Bertoletti correlation had no factor related directly to the ratio of the heated length to the tube bore, but it did include terms for the latent heat of the coolant and its pressure.

Expressed in c.g.s. units, the correlation was originally given as:

$$PHIC = \frac{0.417 H_g}{[(P_{cr}/P)-1]^{0.4}\, D^{0.4}} \left[\frac{1 - (P/P_{cr})}{(G/100)^{1/3}} - X \right]$$

In his work on transient post-dryout heat transfer characteristics, Green [1978] compared his experimental CHF values with those predicted by the Bertoletti equation and found that better agreement was achieved by changing the exponent of the tube diameter to a value of 0.5 and reducing the quality by an arbitrary 10 per cent. Both the modified version of the Bertoletti correlation and the original are compared with the data in the present work.

3. EXPERIMENTAL EQUIPMENT AND OPERATING PROCEDURE

Since a detailed description of the Freon-12 test facility (Figure 1) was given by Ilic [1972], only components and operations relevant to the present work are discussed in this report.

The flow was monitored by means of a turbine flowmeter which had been calibrated to an accuracy of ± 0.25 per cent by the manufacturer for the flow range 0.275 to 1.43 $m^3\ h^{-1}$. Further calibration extended the range down to 0.16 $m^3\ h^{-1}$, but the accuracy at lower flow rates was only ± 2 per cent. The flowmeter was positioned upstream of an 80 kW preheater (see Figure 1) which, in conjunction with a 30 kW chiller unit, controlled the temperature of the coolant at the inlet to the test section. Pressure at inlet to the test section was maintained constant to within ± 5 kPa by an automatically controlled pressuriser unit with a 3 kW heater. Fluid temperatures were measured by resistance thermometers located immediately upstream and downstream of the test section.

Each test section consisted of a stainless steel round tube which was heated over two sections (see Figure 2) by passing direct current along the tube wall. Three test sections were used, their dimensions being given on Figure 2. Five 1 mm diameter stainless steel sheathed, chromel-alumel thermocouples having insulated hot junctions, were attached to the outer wall of each test section. Positions of the thermocouples are shown in Figure 2. The output from the thermocouples was fed to a 200-gain multichannel amplifier and then to a six-channel recorder. For ease of rig operation, the sixth channel of the recorder was arranged to monitor the voltage drop over the main test section (i.e. section (A)). However, to determine the power inputs, the voltage drops and currents over each test section were recorded independently

on a data logging system. In the case of the current measurements, these were obtained by determining the voltage drops across calibrated resistance shunts.

At the start and end of each day's experimentation, heat balance tests were made to ensure that the rig instrumentation was functioning correctly. These heat balance runs were performed at constant coolant flow rate, constant inlet temperature and constant pressure, with the coolant exit temperature several degrees below boiling. The heat balance was acceptable as long as the measured rate of fluid energy gain through the test section, as determined from the mass flow rate and temperature rise over the test section, was within three per cent of test section electrical power input.

Having first set the coolant inlet conditions (mass flow rate, temperature and pressure), the following test procedure was followed:

(1) Trial runs were performed to establish approximate power inputs at dryout.

(2) With little or no power on the short section of the heated length (B), the power on the main section (A) was gradually raised until dryout was obtained at the end of A, i.e. when thermocouple TC5 indicated dryout.

(3) The power on A was then reduced by approximately 1 to 2 per cent to bring it out of dryout and the power to B increased until thermocouples TC1 and TC2 indicated dryout.

(4) Power to B was then lowered until there was no indication of dryout in either test section.

During the above procedure, thermocouples were used to indicate dryout and an electrical bridge burnout detector [see Ilic 1978] was used to indicate burnout on the main test section (Figure 2). A full scan of rig conditions (coolant temperature and pressure at inlet, pressure drop along the test section, coolant flow rate, voltage and current values on each section) was recorded manually and from signals transmitted directly to a data logging system, when each of the four steps had been completed.

A small computer program which contained the properties of Freon-12 was used in conjunction with the observed values of exit pressure, coolant flow

rate, total power and inlet coolant temperature, to evaluate exit qualities (dryness fractions). The accuracy of the computed qualities which are quoted in the appendices is, therefore, dependent on the accuracies to which these quantities could be measured; this was no better than ± 3 per cent.

Midway through the test program, the experimental procedure was varied by subdividing step 3 as follows:

3A The power on A was maintained at the 'just dryout' point and the power on B raised until thermocouples TC1 and TC2 began increasing in temperature, albeit only slowly.

3B Power on A was then lowered by one to two per cent to bring it out of dryout and also cause the wall temperatures at B, indicated by TC1 and TC2, to fall to non-dryout levels. The power on B was then increased until TC1 and TC2 again indicated dryout.

At both of these steps a full scan of rig conditions was taken as before.

The data obtained for dryout conditions in the main test section only, i.e. corresponding to step 2, are tabulated in Appendix A. Data relating to steps 3, 3A and 3B are given in Appendices B, C and D respectively.

Information acquired in step 4 was used only for reference when comparing manually recorded data with signals transmitted directly to the data logging system.

4. ANALYSIS OF EXPERIMENTAL DATA

4.1 General

The experimental procedure used in this work enabled data on dryout to be gathered for both uniformly and non-uniformly heated conditions. The former condition refers to the tests in which dryout was obtained with heating on section A only, and the latter to the tests in which dryout was obtained on section B, where the heat flux was different from that on the upstream section.

4.2 Uniformly Heated Tubes

Initially, the experimental data were compared with values of critical heat flux calculated from each of the three correlations using local coolant conditions at the exit of the test section. Figures 3 to 5 show typical comparisons, which indicate that the modified Groeneveld and modified Bertoletti correlations agree with the experimental data only to within ± 25 per cent, and the Bertoletti correlation is even worse than this. Further scrutiny of the information shown in Figures 4 and 5 indicates that, apart from random variations in the errors between experimental and predicted values, there is a systematic error in the correlations in predicting the effect of the mass flux. To highlight this effect, the ratios of experimental to predicted value of critical heat flux have been plotted against mass flux in Figures 6 to 11.

Another discrepancy between predicted and experimental values is discernible from these figures. Whereas the Bertoletti and modified Bertoletti correlations include a parameter (P/P_{cr}) to account for the effect of coolant pressure, the Groeneveld correlation makes no such allowance. As can be seen from Figures 6 and 9, the Groeneveld correlation is erroneous in this respect.

4.3 Non-uniformly Heated Tubes

Comparison of experimental values of critical heat flux with values obtained from each of the correlations showed that the correlations were unsuitable for predicting local CHFs under such conditions. Typical examples of the comparisons obtained for the 8.48 mm bore tube are shown in Figures 12, 13 and 14. These figures show that although CHF values obtained from either the modified Groeneveld or modified Bertoletti correlations in general underpredict the observed values, predicted values cover only a relatively small range of CHFs while experimental CHFs cover a much wider range. These comparisons also indicate that the differences between predicted and experimental values are a function of mass flux. Data shown on Figures 12 to 14 have been taken from Appendices B and D.

5. EXAMINATION OF PUBLISHED CHF DATA

5.1 Data from Overseas Freon-12 Facilities

Groeneveld [1969] has presented information obtained from uniformly heated tubes cooled by Freon-12, the ranges of the experimental conditions investigated being given in Table 1. These experimental data are compared with the modified Groeneveld and both versions of the Bertoletti correlation in Figures 15 to 17; the modified Groeneveld equation correlates best with the data, the modified Bertoletti equation being somewhat better than the original Bertoletti correlation, at least for the low mass fluxes.

It should be noted that all of the experimental data given by Groeneveld for values of exit quality equal to or above zero have been included. Groeneveld considered data outside the range 0.05 to 0.7 to be in "different flow regimes" and excluded them. This exclusion is the reason that the error between the CHF values predicted by the Groeneveld correlation and corresponding experimental values is greater than that reported by Groeneveld. However, there is no evidence of the wide variations mentioned by Groeneveld.

With both the Bertoletti and modified Bertoletti correlations, the variation between predicted and experimental CHF values is considerably greater than that obtained with the Groeneveld equation. The Bertoletti correlation consistently underpredicts the CHF values, but although the modified version has an improved average error, the range of error is greater. All three comparisons indicate, however, that there appears to be no consistent relationship between the ratio of predicted to experimental values of CHF and mass flux.

About some ten years later, apparently using the same experimental facilities as Groeneveld, Merilo and Ahmad [1979] obtained dryout data for both vertical and horizontal uniformly heated tubes. The ranges of experimental conditions investigated by these experimenters are given in Table 1. In contrast to Groeneveld, Merilo and Ahmad used a range of outlet pressures and a larger range of mass fluxes. Their data from vertical tubes have been considered in the same manner as those used for the Groeneveld correlation. This shows that, as was expected, when the experimental data are compared with the Groeneveld correlation data, the correlation is quite erroneous for mass fluxes greater than 4400 kg m^{-2} s^{-1} (for these mass fluxes negative CHFs are predicted) and for data in the mass flux range 1000 to 3000

kg m^{-2} s^{-1}, it generally overestimates the experimental values. There are indications, however, that with increasing mass flux this overestimation decreases. For data within the range 3000 to 4000 kg m^{-2} s^{-1}, this trend continues so that the experimental CHFs become 50 to 100 per cent higher than the predicted values. In this mass flux range, the accuracy of the correlation is questionable.

Comparison of the same data with the predicted values from the Bertoletti and modified Bertoletti correlations shows that the ratio of experimental to predicted CHF increases as mass flux increases, but with increasing scatter at the higher mass fluxes. Furthermore, for mass fluxes above 7000 kg m^{-2} s^{-1}, the experimental data may be up to 500 per cent higher than predicted values.

Both the Bertoletti and modified Bertoletti correlations contain a factor of the form

$$\left[\frac{(1-P/P_{cr})}{(G/100)^{1/3}} - A\,X_o\right]$$

where A = 1 for the Bertoletti correlation, A = 0.9 for the modified version.

Such a factor can obviously cause incorrect predictions of critical heat fluxes if the negative part exceeds the positive part. This could happen at high mass fluxes and high exit qualities. Merilo and Ahmad's data encompass such conditions and, under certain high mass flux and high exit quality conditions, these correlations give negative values. This occurred for a small number of data. The increasing scatter observed at high mass fluxes may also be attributed to this deficiency.

Apart from these effects, it would appear that all three correlations adequately represent the effects of tube bore, but while the Bertoletti and modified Bertoletti correlations take account of coolant pressure, the Groeneveld correlation does not.

5.2 Earlier AAEC Data

Stevens and Miles [1980], using the AAEC Freon-12 facility, obtained data on critical heat flux for three uniformly heated tubes. A limited pressure range was investigated but ranges of mass flux and exit quality were wider (Table 1).

Comparison of the Stevens and Miles data with those of the Groeneveld, Bertoletti and modified Bertoletti correlations shows that the trends and magnitudes of CHF ratios are similar to those obtained using the Merilo and Ahmad [1979] data and the most recent AAEC data. That is to say, the Groeneveld correlation does not account for the effect of pressure and there is an increasing disparity between values predicted by all three correlations and experimental data at high mass fluxes. These comparisons are shown in Figures 18 to 20.

6. DISCUSSION

6.1 Uniformly Heated Tubes

Ratios of experimental to predicted critical heat flux for uniformly heated tubes increase as the mass flux increases for all three correlations. Furthermore it has been found that even in the range of experimental conditions for which the correlations appear to be best suited, their accuracy is only ± 20 per cent. Also the modified Groeneveld correlation should not be used with mass fluxes greater than 3500 kg m^{-2} s^{-1} and is incapable of allowing for the effect of pressure. The Bertoletti correlation, apart from defects at high mass fluxes, also exhibits increasing inaccuracies at low mass fluxes (i.e. mass fluxes less than 750 kg m^{-2} s^{-1}).

6.2 Non-uniformly Heated Tubes

The assumption that thermal equilibrium and cross-sectional average coolant conditions are sufficient to enable local critical heat fluxes to be calculated is frequently used when attempting to predict the transient thermal performance of a nuclear reactor fuel element subjected to a loss-of-coolant accident. Tests of the type performed in the present work, i.e. with a discontinuity in the axial distribution of heat flux, are particularly apt for critically investigating such an assumption.

Comparison of the data obtained on local critical heat fluxes from these experiments with values predicted by the three correlations showed that such data could not be predicted by any of the correlations. Bearing in mind that these correlations were not very accurate in predicting the uniformly heated data, this observation nevertheless implies that local critical heat fluxes cannot be determined for a particular fluid and channel from only a knowledge

of cross-sectional average values of coolant mass flux, pressure and quality. This conclusion concurs with views stated by Stevens, Elliott and Wood [1965], who used a similar experimental approach to that presented in this work, except that they used a 'hot patch' technique in which the short end section had an average heat flux approximately twice that of the main tube. In their experimental arrangement, when power to the hot patch was increased, it was also increased in the main section. Using this technique, Stevens et al. [1965] concluded that the local conditions hypothesis "cannot be regarded as valid even in the high quality regions where it appears to work so well". Stevens et al. also found that, for apparently the same local coolant conditions, the experimental critical heat fluxes of the hot patch were higher than those occurring at the exit of a uniformly heated tube.

Although this observation appears to be at variance with our results, where the critical heat fluxes are mostly much lower in the separately heated section, they are consistent with the Harwell model of liquid film dryout for two-phase annular flow conditions [Hewitt and Hall-Taylor 1970]. With this concept, droplet deposition and evaporation would be the significant mechanisms for the onset of dryout with the non-uniform heating conditions used in this work. When the main part of the test section is subjected to a heat flux just below that which would induce dryout, the local heat flux in the short exit section need only be slightly more than that required to balance the droplet deposition, and dryout ensues. Our results appear qualitatively to substantiate this concept.

The problem remains, however, that in many loss-of-coolant accident calculation codes, CHF correlations developed from data for uniformly heated conditions are used to determine the onset of dryout and, as this experimental work has shown, such calculated values can be significantly different from the local critical heat fluxes obtaining in non-uniformly heated situations.

7. CONCLUSIONS

The Bertoletti, modified Groeneveld and modified Bertoletti correlations, although specifically developed for predicting critical heat fluxes in uniformly heated tubes cooled by Freon-12, are generally no better than ± 20 per cent for these conditions.

The experimental data obtained from non-uniformly heated tubes qualitatively substantiate the concept of droplet deposition-controlled dryout and highlight the fact that empirical correlations developed from data for uniformly heated tubes are unsuitable for prediction of the onset of dryout with non-uniform heating.

8. ACKNOWLEDGEMENTS

The authors express their thanks to Mr C. Evans for preparing the experimental data for graphical analysis.

9. REFERENCES

Barnett, P.G. [1963] - An investigation into the validity of certain hypotheses implied by various burnout correlations. AEEW-R214.

Becker, K.M. [1965] - An analytical and experimental study of burnout conditions in vertical round ducts. A.B. Atomenergi Report AE-178.

Bertoletti, S., Gaspari, F.P., Lombardi, C., Peterlongo, G. and Tacconi, F.A. [1964] - Heat transfer crisis with steam-water mixtures. CISE R99.

Biasi, L., Clerici, G.C., Garriba, S., Sala, R. and Tozzi, A. [1967] - A new correlation for round duct and uniform heating - comparison with world data. EUR 3376e.

Bowring, R.W. [1972] - A simple but accurate round tube, uniform heat flux, dryout correlation over the pressure range 0.7 to 17 MN/m^2. AEEW-R789.

Green, W.J. [1978] - An experimental and analytical study of transient heat transfer in the region of dryout for a heated tube using Freon-12 as coolant. AAEC/E452.

Green, W.J. and Lawther, K.R. [1979] - An investigation of transient heat transfer in the region of flow boiling dryout with Freon-12 in a heated tube. Nucl. Eng. Des., 55:131-144.

Green, W.J. and Lawther, K.R. [1980] - An experimental study of dryout heat transfer in tubes by a temperature transient method. Session 15, ANS-ASME Topical Meeting on Nuclear Reactor Thermohydraulics, Saratoga Springs, New York. (Proceedings to be published).

Groeneveld, D.C. [1969] - Freon dryout correlations and their applicability to water. AECL-3418.

Hewitt, G.F. and Hall-Taylor, N.S. [1970] - Annular two-phase flow. Pergamon Press, Oxford.

Ilic, V. [1972] - The AAEC Freon rig ACTOR and initial boiling crisis (burnout) results. AAEC/TM632.

Katto, Y. [1978] - A generalised correlation of critical heat flux for the forced convection boiling in vertical uniformly heated round tubes. Int. J. Heat Mass Transfer, 21:1527-1542.

Merilo, M. and Ahmad, S.Y. [1979] - The effect of diameter on vertical and horizontal flow boiling crisis in a tube cooled by Freon-12. AECL-6485.

Roko, K., Takitani, K., Yoshizaki, A. and Shiraha, M. [1978] - Dryout characteristics at low mass velocities in a vertical straight tube of a steam generator. Proc. 6th Int. Heat Transfer Conference, Toronto, Vol.1, pp.429-434.

Shah, M.M. [1978] - A generalised graphical method for predicting CHF in uniformly heated tubes. Int. J. Heat Mass Transfer, 22:557-560.

Stevens, G.F., Elliot, D.F. and Wood, R.W. [1964] - An experimental investigation into forced convection burnout in Freon, with references to burnout in water. AEEW-R321.

Stevens, G.F., Elliot, D.F. and Wood, R.W. [1965] - An experimental comparison between forced convection burnout in Freon-12 flowing vertically upwards through uniformly heated round tubes. AEEW-R426.

Stevens, J.R. and Miles, D.N. [1980] - Boiling crisis data for vertical upflow of Freon-12 in round tubes and annuli. AAEC/E506.

Thompson, B. and Macbeth, R.V. [1964] - Boiling water heat transfer - burnout in uniformly heated round tubes: A compilation of world data with accurate correlations. AEEW-R356.

10. NOTATION

b	numerical constant in Groeneveld correlation
CHF	critical heat flux
D	tube bore
G	mass flux
H_g	latent heat of vaporisation
L	heated length
PHIC	CHF predicted by Bertoletti correlation
PHICMD	CHF predicted by modified Bertoletti correlation
PHIG	CHF predicted by modified Groeneveld correlation
P	coolant pressure
P_{cr}	critical pressure
X	mass fraction (quality)

TABLE 1

EXPERIMENTAL CONDITIONS FOR VARIOUS CHF INVESTIGATIONS

Source of Data	Outlet Pressure (MPa)	Mass Flux ($kg\ m^{-2}\ s^{-1}$)	Heat Flux ($kW\ m^{-2}$)	Inlet Subcooling ($kJ\ kg^{-1}$)	Outlet Quality	Tube Diameter (mm)	Heated Length (mm)
Groeneveld [1969]	1.05	500	60	0	-0.06	7.8	610
	to	to	to	to	to	10.9	to
	1.10	3255	271	30.0	0.79	16.1	1829
Merilo and Ahmad [1979]	1.00	1500	38	-4.2	0.013	5.3	1030
	1.28	to	to	to	to		to
	1.52	8600	417	40.0	0.764	12.6	4880
Stevens and Miles [1980]	0.96	450	62	2.8	0.007	15.34	2850
	to	to	to	to	to	16.08	to
	1.05	3850	193	35.0	0.784	21.54	3940
Green and Stevens [1981]	0.90	380	55	0.26	0.19	8.48	2870
	to	to	to	to	to	16.76	to
	1.32	2800	128	41.0	0.86	21.34	3700

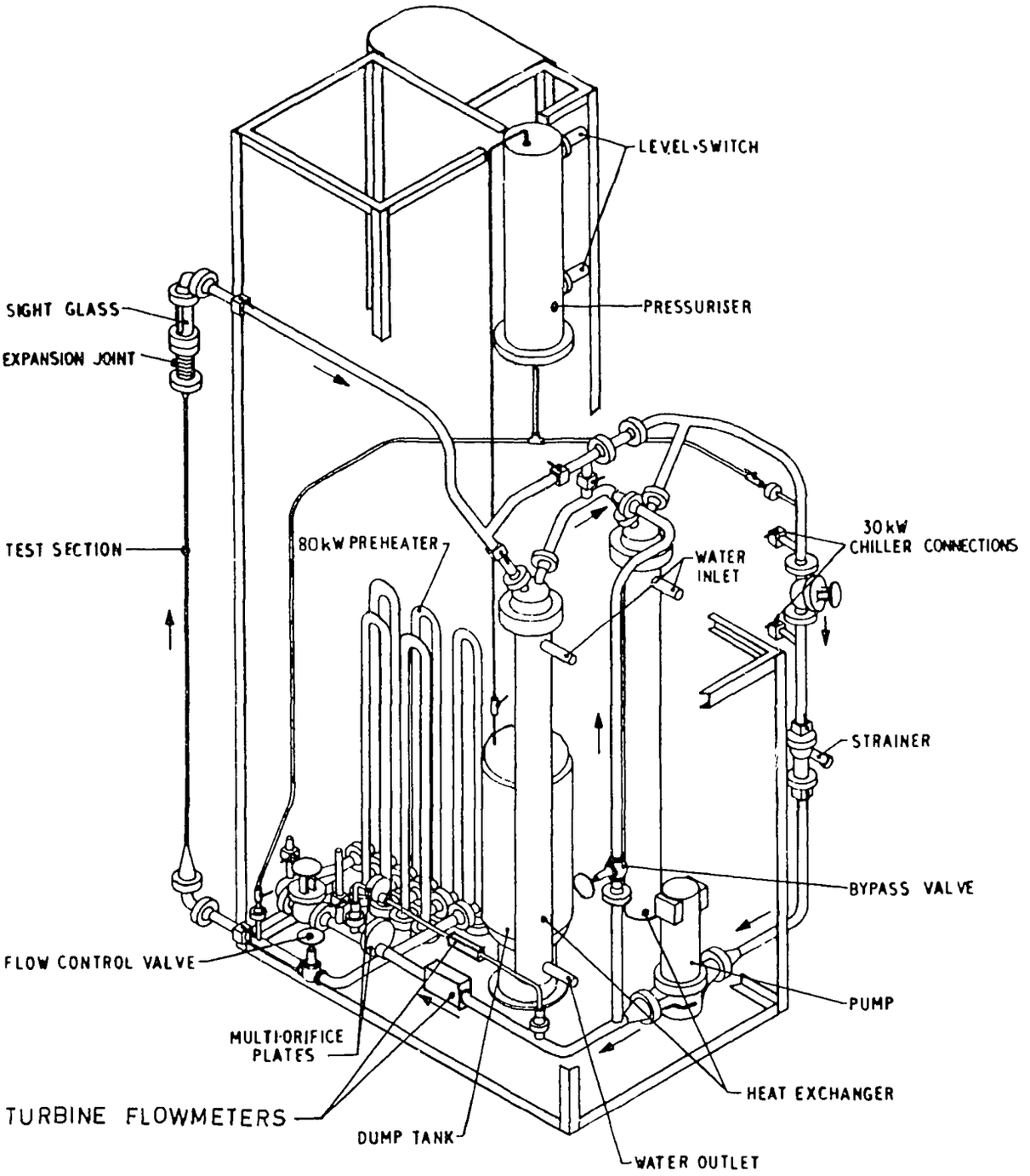

FIGURE 1. ISOMETRIC VIEW OF THE FREON LOOP ACTOR

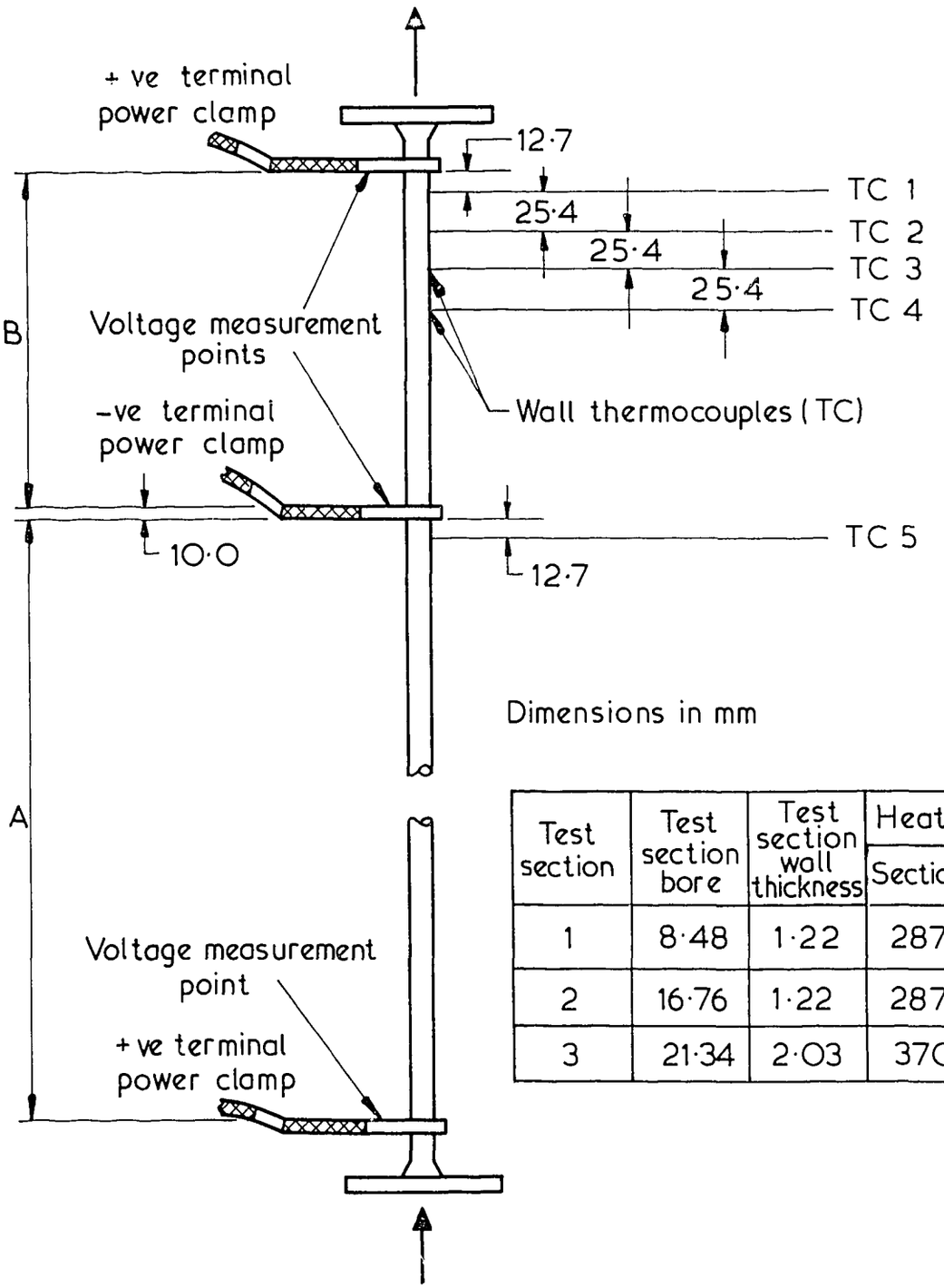

Test section	Test section bore	Test section wall thickness	Heated length	
			Section A	Section B
1	8·48	1·22	2870	230
2	16·76	1·22	2870	230
3	21·34	2·03	3700	230

FIGURE 2. TEST SECTION INSTRUMENTATION

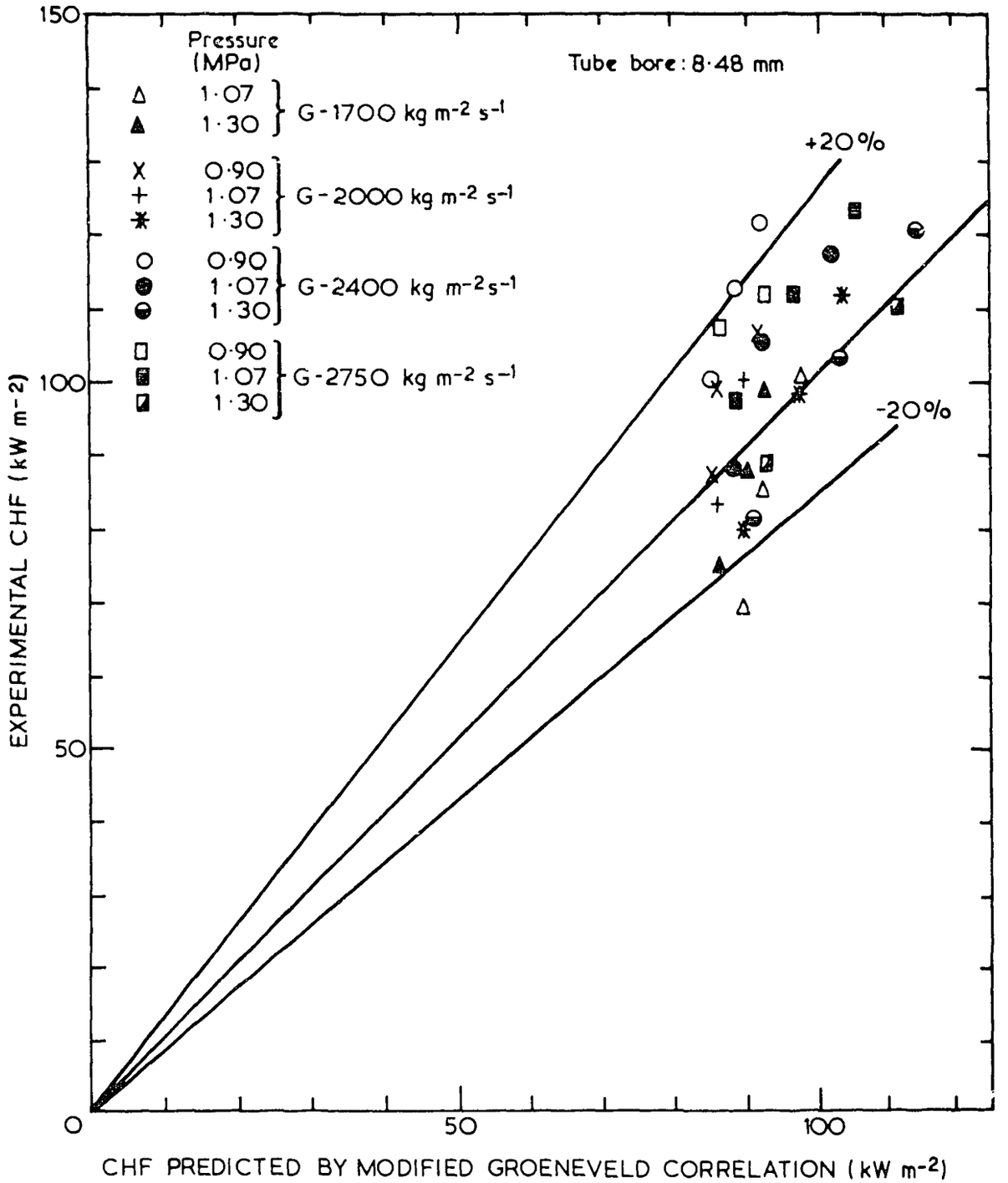

FIGURE 3. COMPARISON OF EXPERIMENTAL CHFs AT THE END OF A UNIFORMLY HEATED TUBE WITH VALUES PREDICTED BY THE MODIFIED GROENEVELD CORRELATION

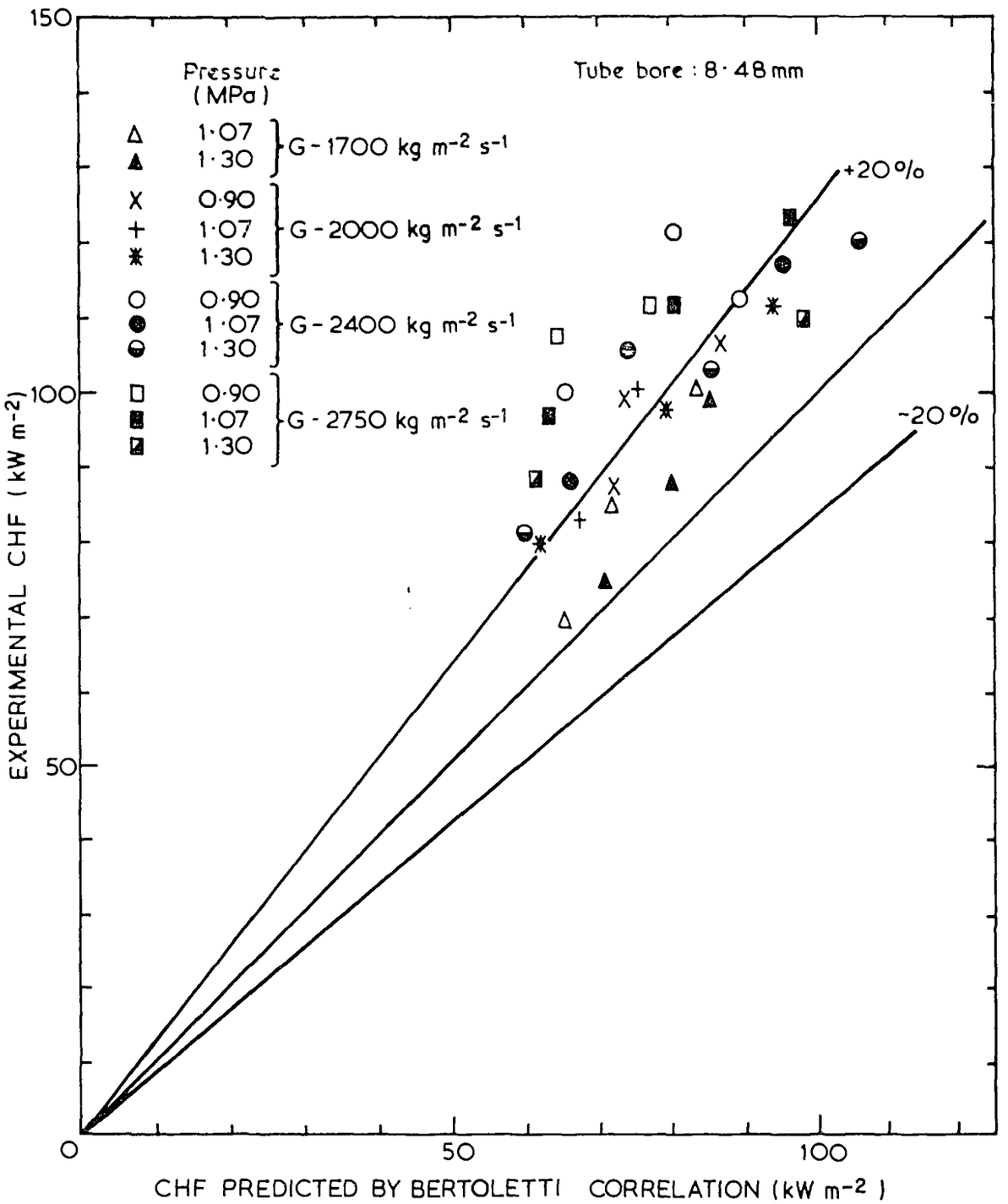

FIGURE 4. COMPARISON OF EXPERIMENTAL CHFs AT THE END OF A UNIFORMLY HEATED TUBE WITH VALUES PREDICTED BY THE BERTOLETTI CORRELATION

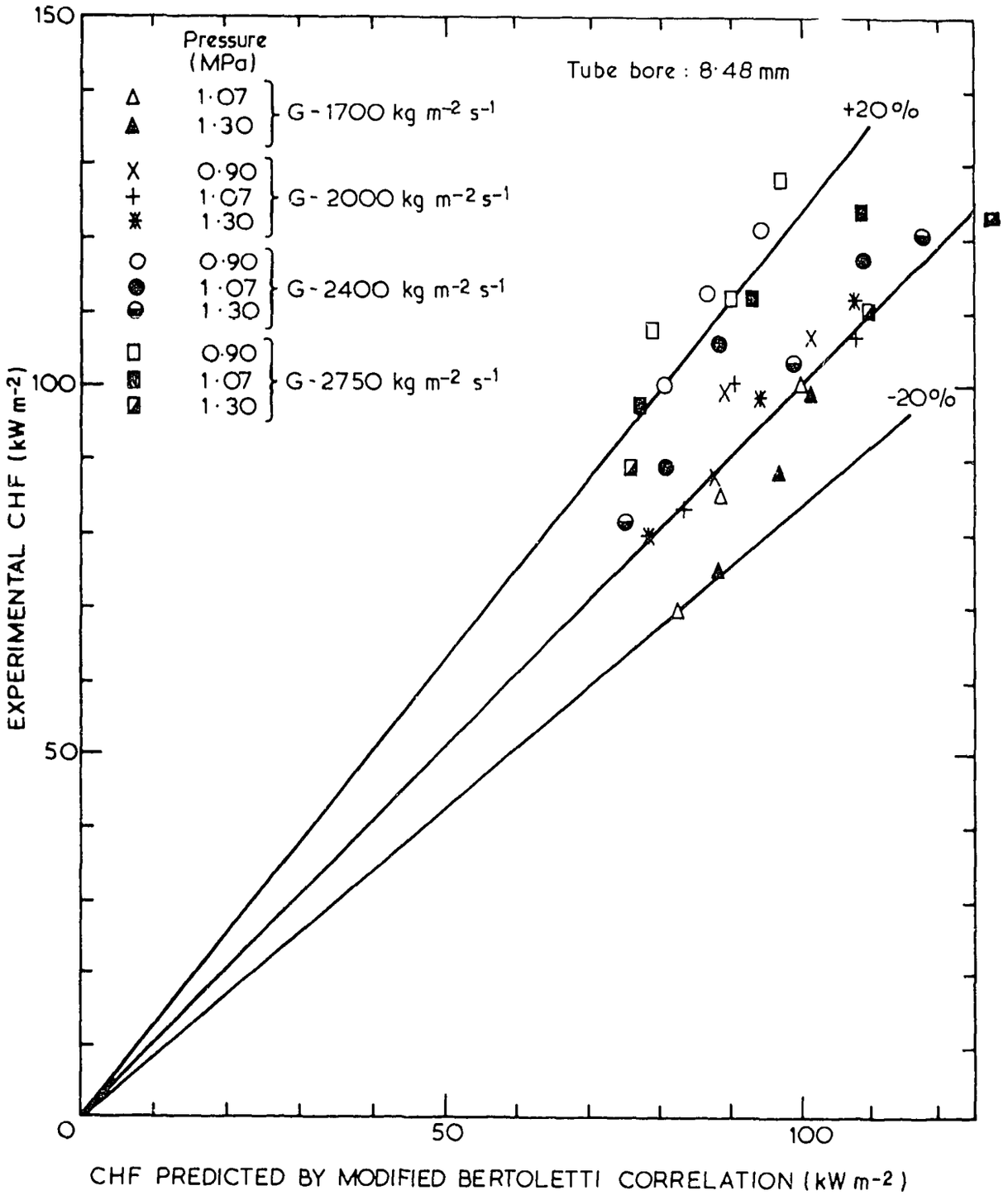

FIGURE 5. COMPARISON OF EXPERIMENTAL CHFs AT THE END OF A UNIFORMLY HEATED TUBE WITH VALUES PREDICTED BY THE MODIFIED BERTOLETTI CORRELATION

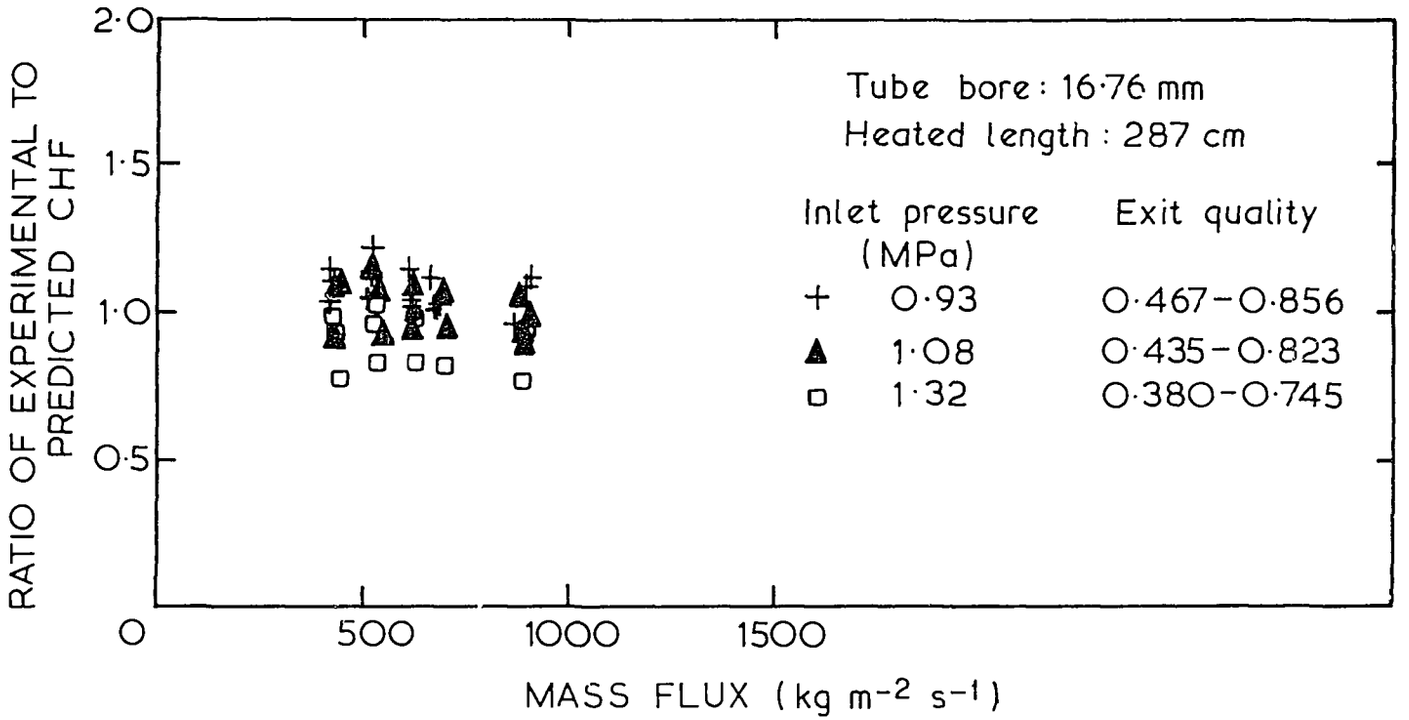

FIGURE 6. RATIO OF EXPERIMENTAL TO PREDICTED CHFs VERSUS MASS FLUX AT THE EXIT OF A UNIFORMLY HEATED TUBE USING THE MODIFIED GROENEVELD CORRELATION

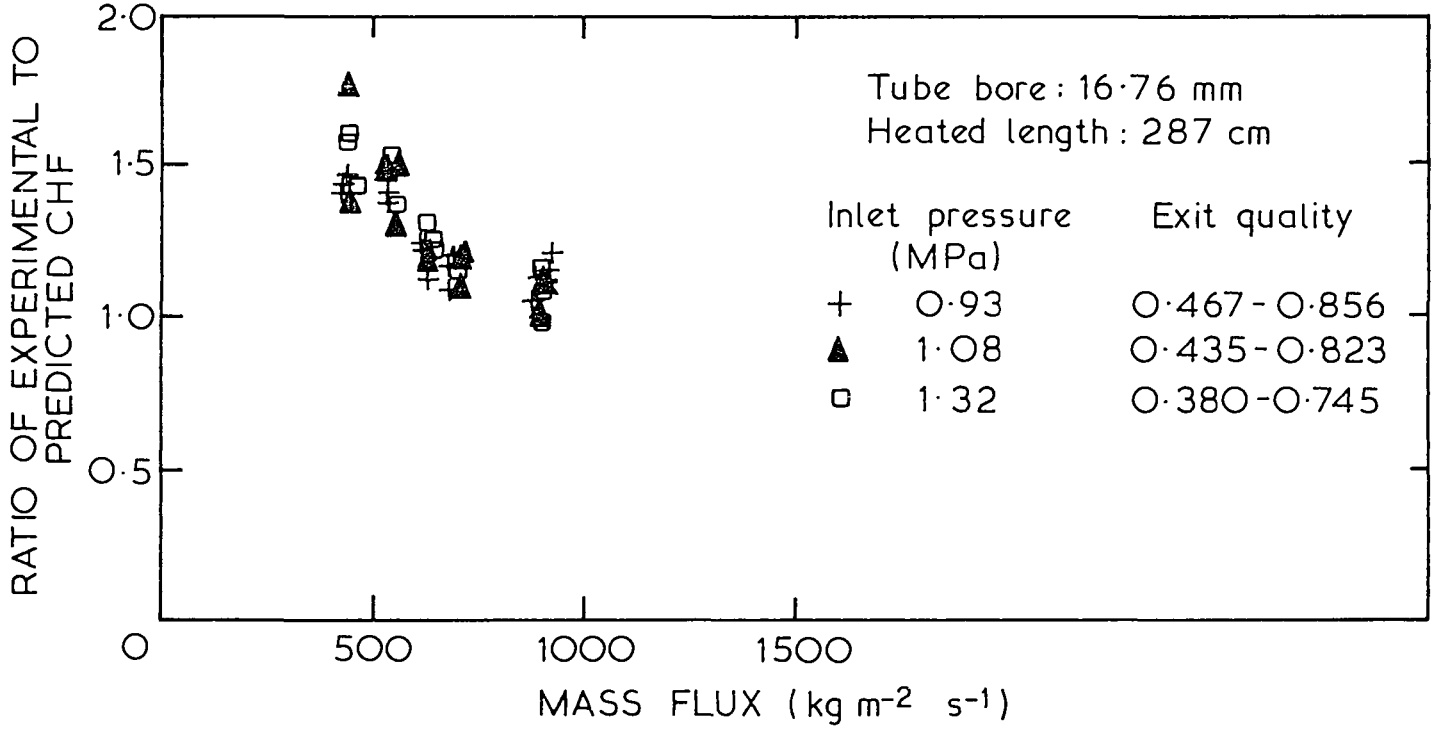

FIGURE 7. RATIO OF EXPERIMENTAL TO PREDICTED CHFs VERSUS MASS FLUX AT THE EXIT OF A UNIFORMLY HEATED TUBE USING THE BERTOLETTI CORRELATION

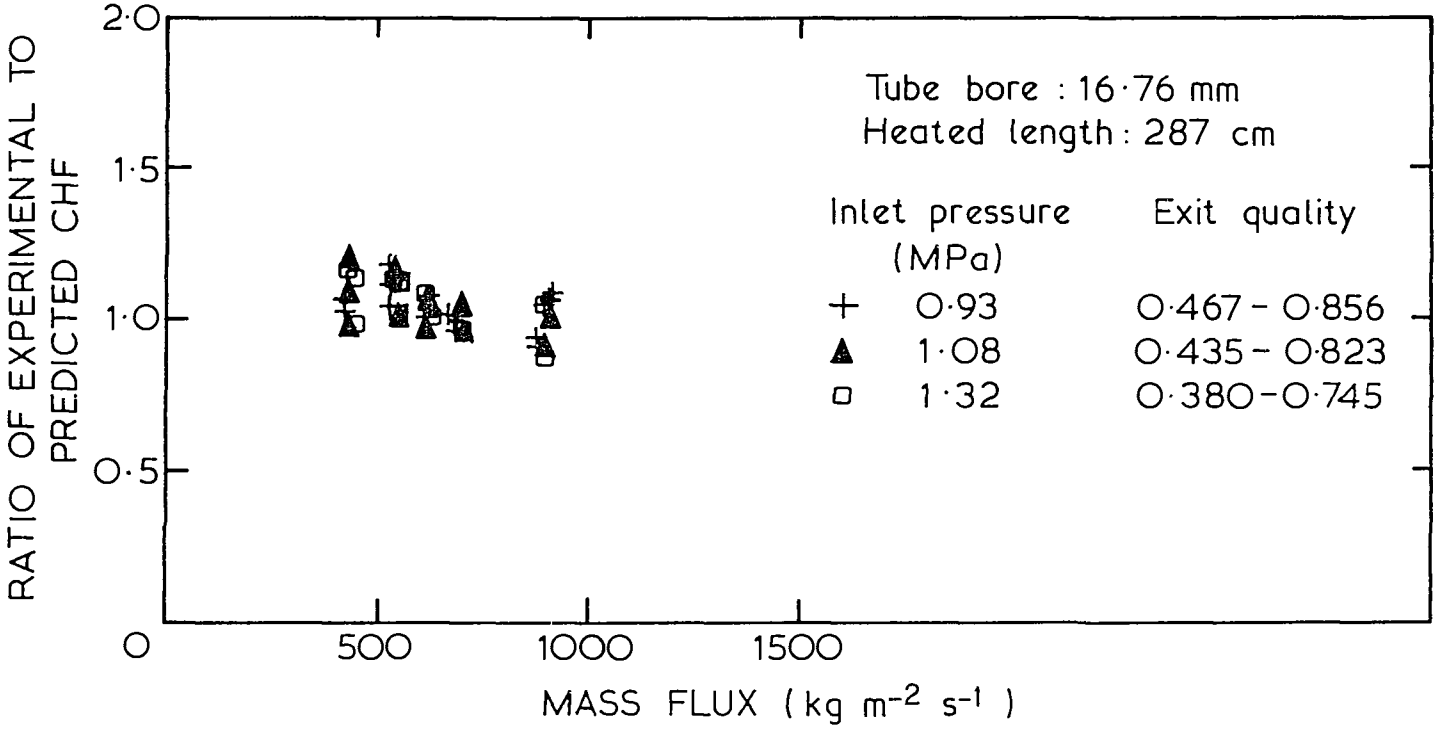

FIGURE 8. RATIO OF EXPERIMENTAL TO PREDICTED CHFs VERSUS MASS FLUX AT THE EXIT OF A UNIFORMLY HEATED TUBE USING THE MODIFIED BERTOLETTI CORRELATION

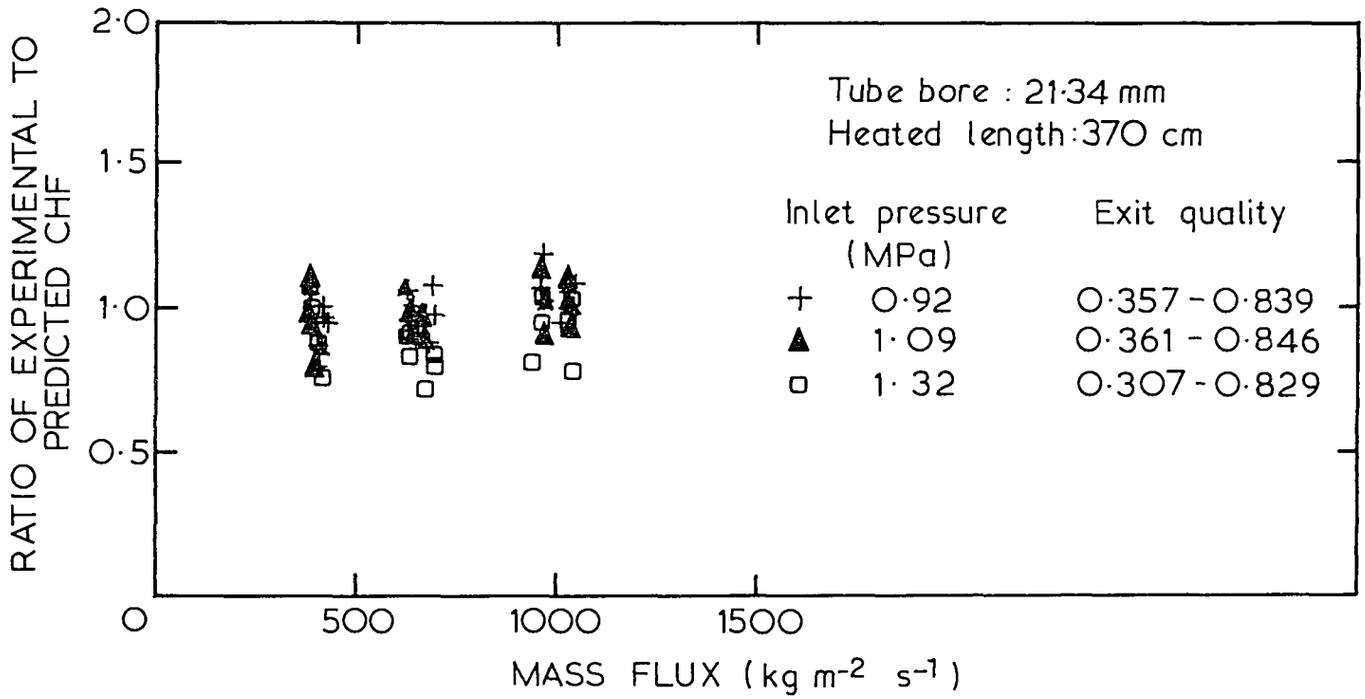

FIGURE 9. RATIO OF EXPERIMENTAL TO PREDICTED CHFs VERSUS MASS FLUX AT THE EXIT OF A UNIFORMLY HEATED TUBE USING THE MODIFIED GROENEVELD CORRELATION

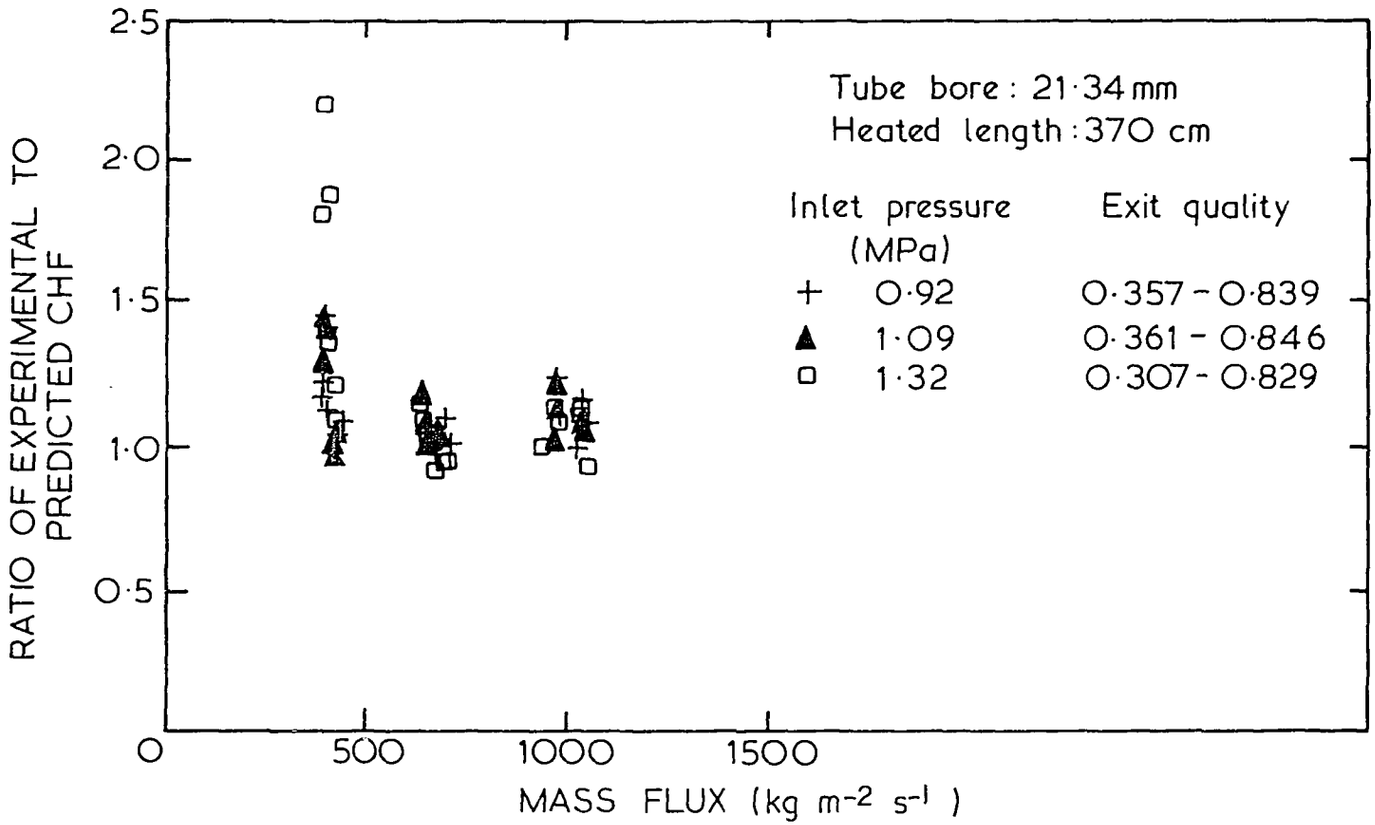

FIGURE 10. RATIO OF EXPERIMENTAL TO PREDICTED CHFs VERSUS MASS FLUX AT THE EXIT OF A UNIFORMLY HEATED TUBE USING THE BERTOLETTI CORRELATION

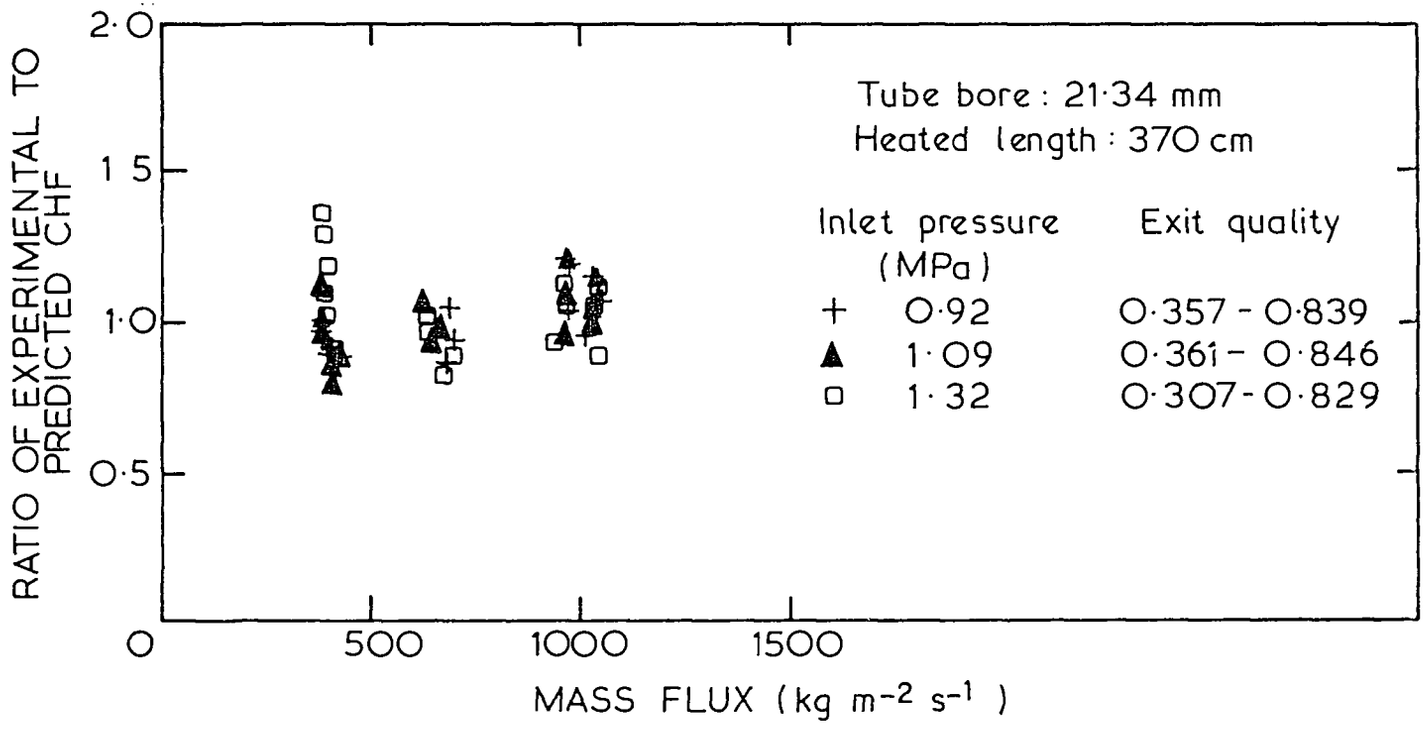

FIGURE 11. RATIO OF EXPERIMENTAL TO PREDICTED CHFs VERSUS MASS FLUX AT THE EXIT OF A UNIFORMLY HEATED TUBE USING THE MODIFIED BERTOLETTI CORRELATION

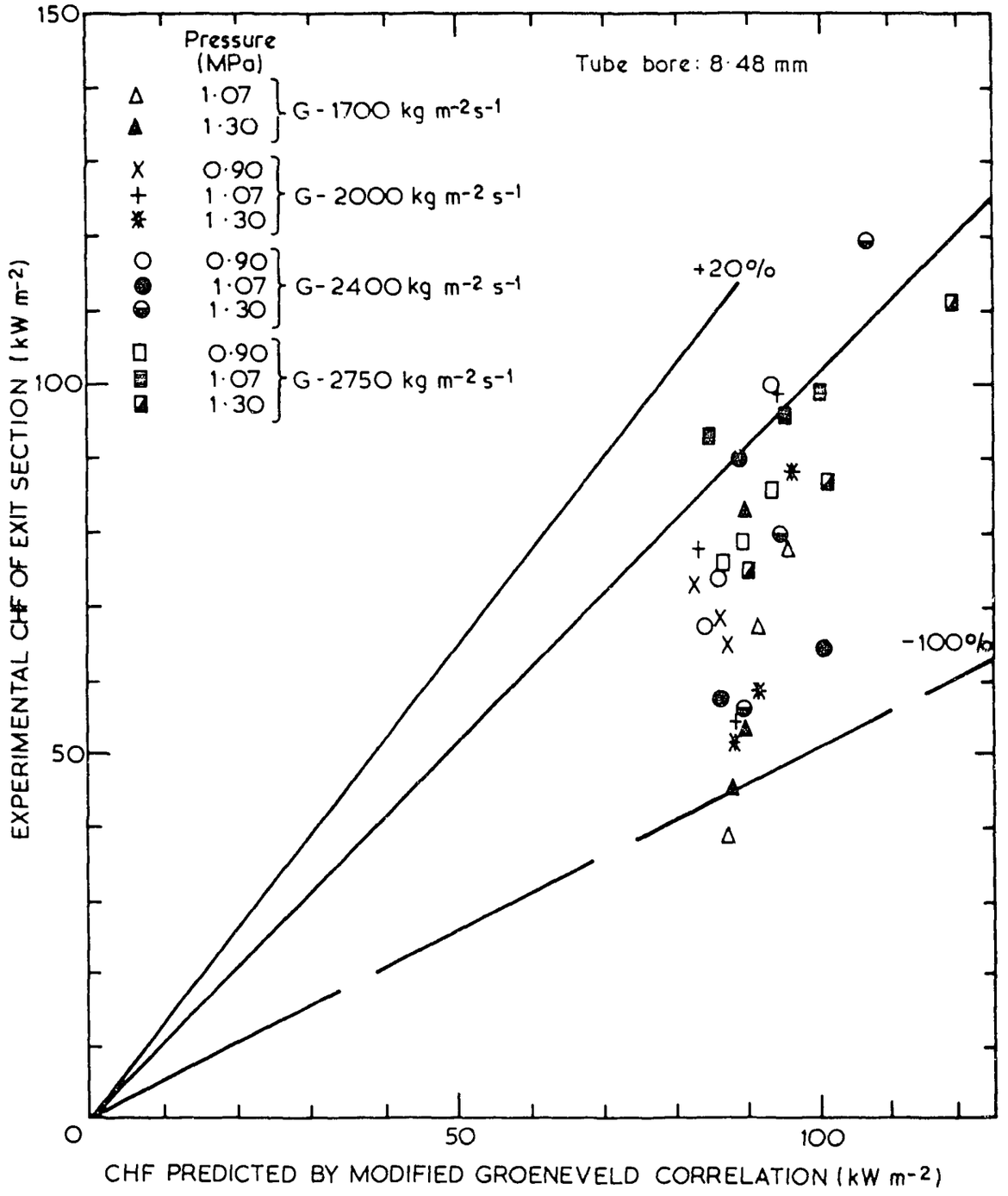

FIGURE 12. COMPARISON OF EXPERIMENTAL CHFs OF EXIT SECTION WITH VALUES PREDICTED BY THE MODIFIED GROENEVELD CORRELATION

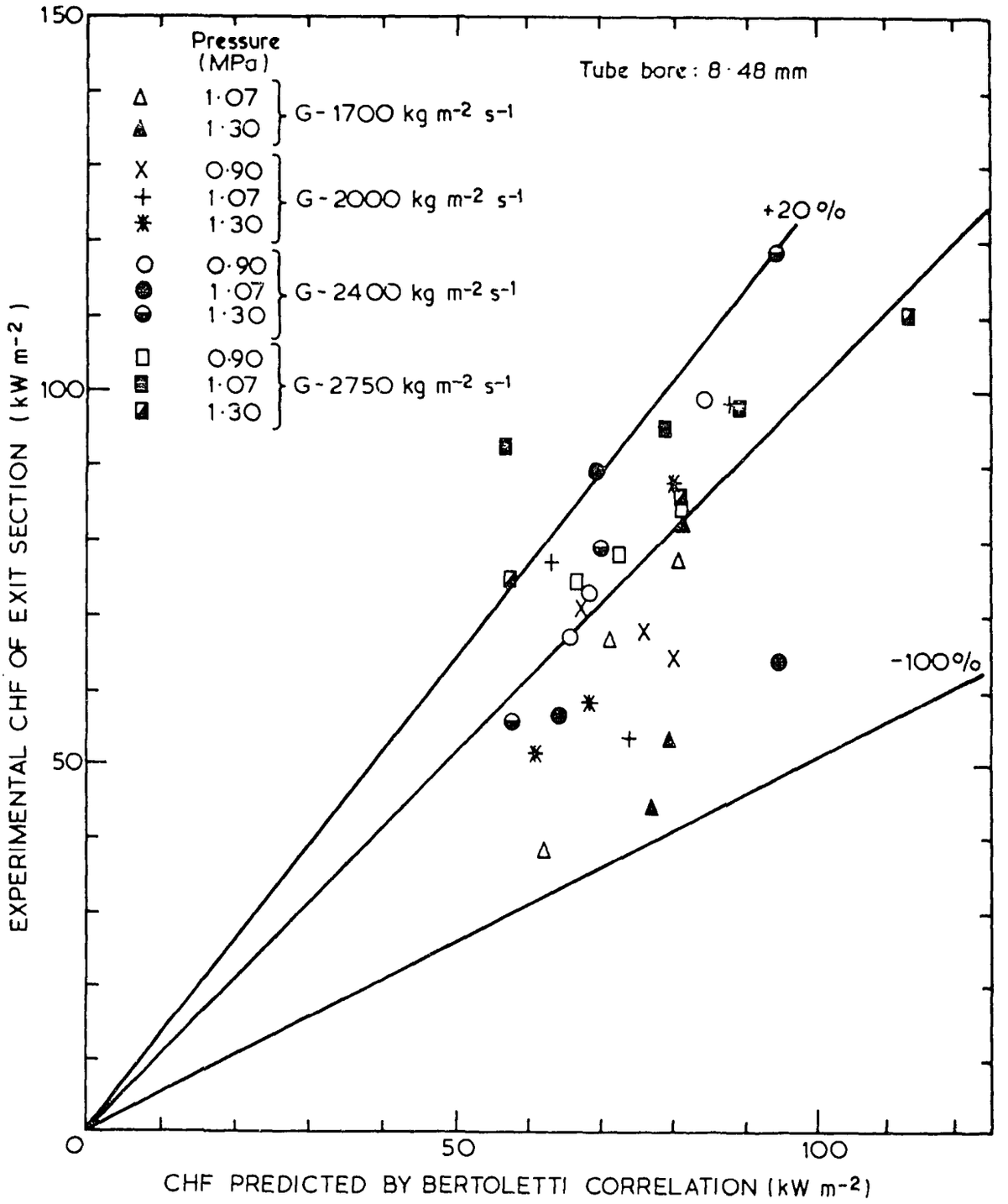

FIGURE 13. COMPARISON OF EXPERIMENTAL CHFs OF EXIT SECTION WITH VALUES PREDICTED BY THE BERTOLETTI CORRELATION

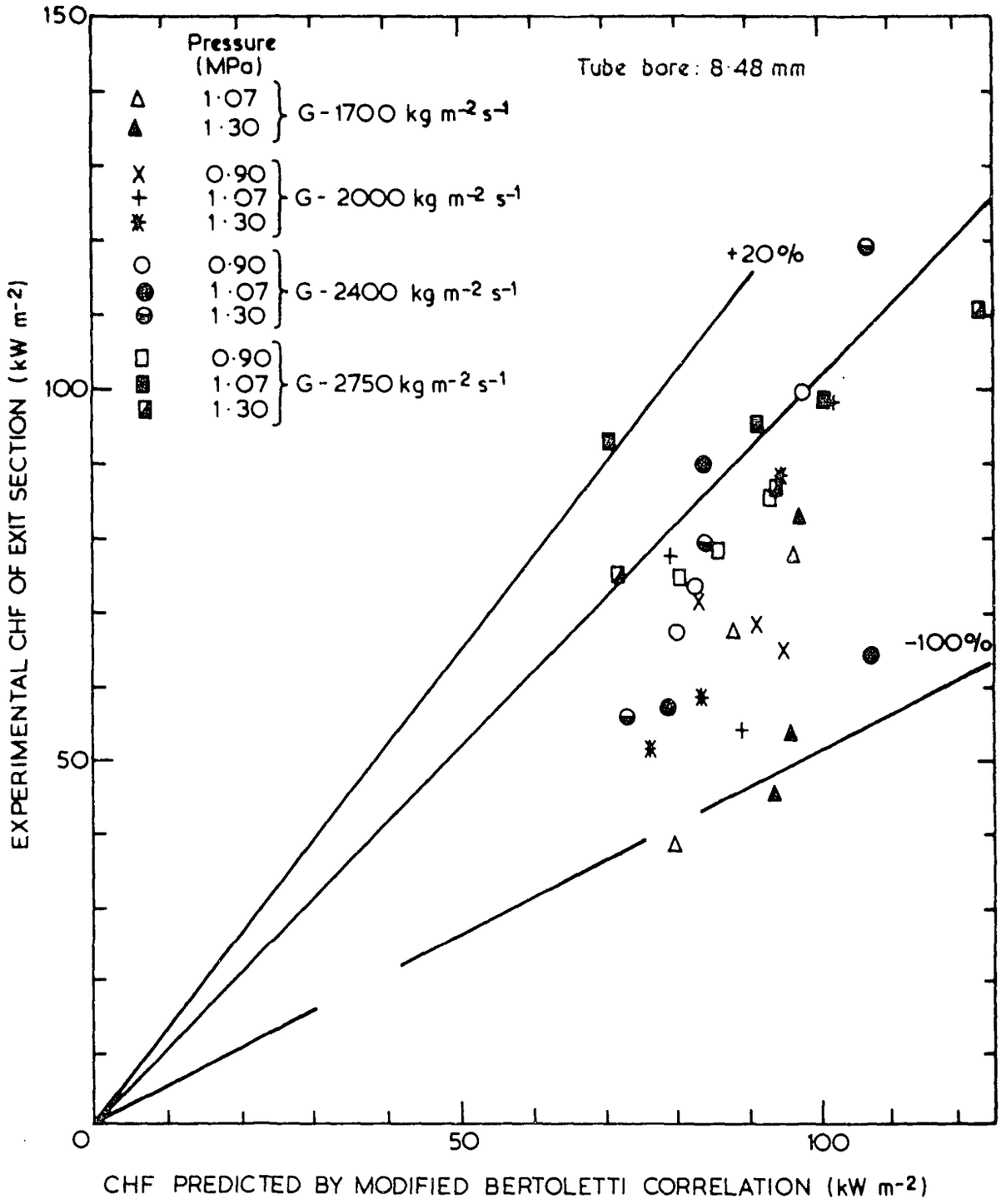

FIGURE 14. COMPARISON OF EXPERIMENTAL CHFs OF EXIT SECTION WITH VALUES PREDICTED BY THE MODIFIED BERTOLETTI CORRELATION

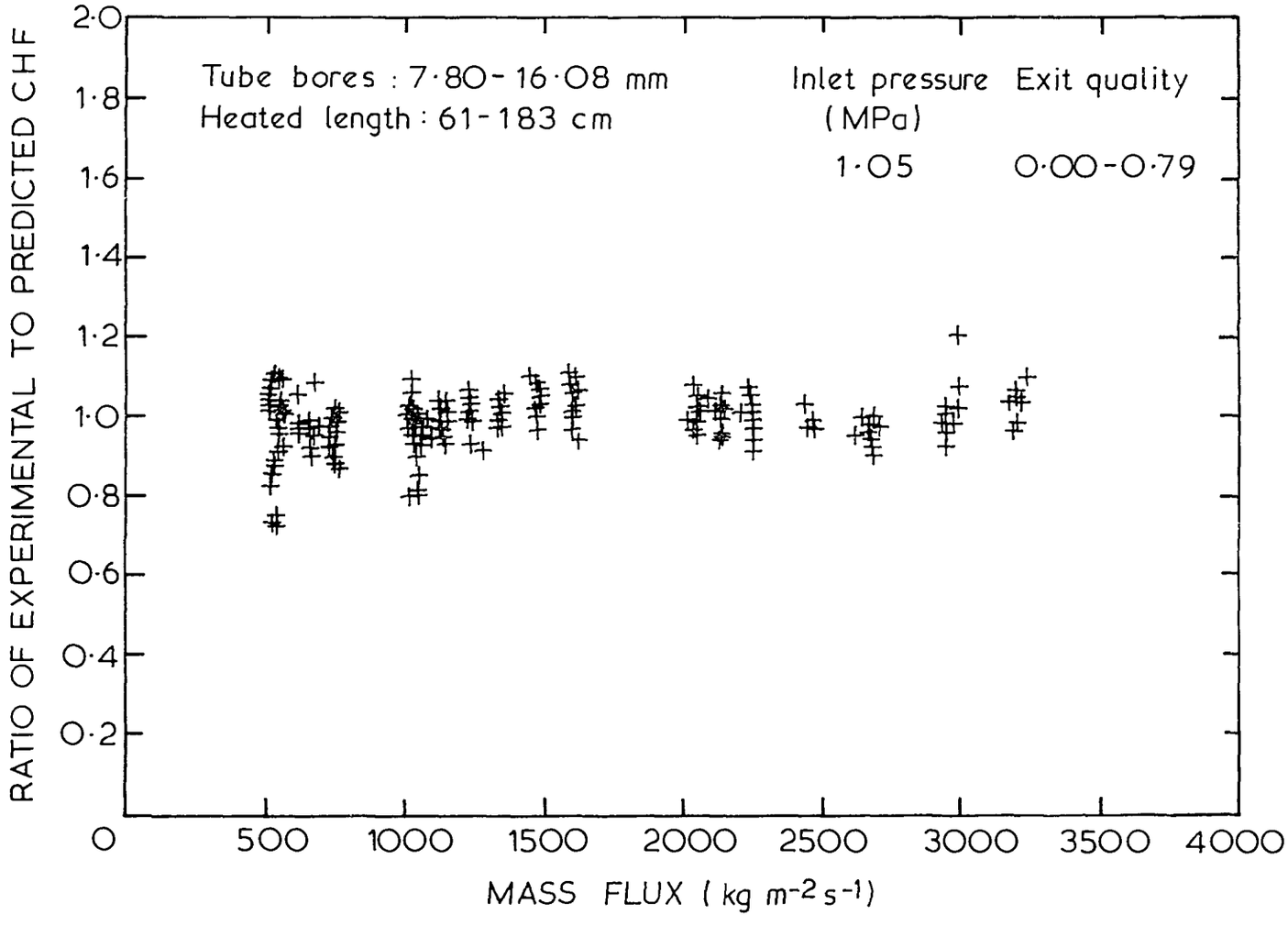

FIGURE 15. RATIO OF EXPERIMENTAL TO PREDICTED CHFs VERSUS MASS FLUX AT THE EXIT OF A UNIFORMLY HEATED TUBE USING THE MODIFIED GROENEVELD CORRELATION (GROENEVELD DATA)

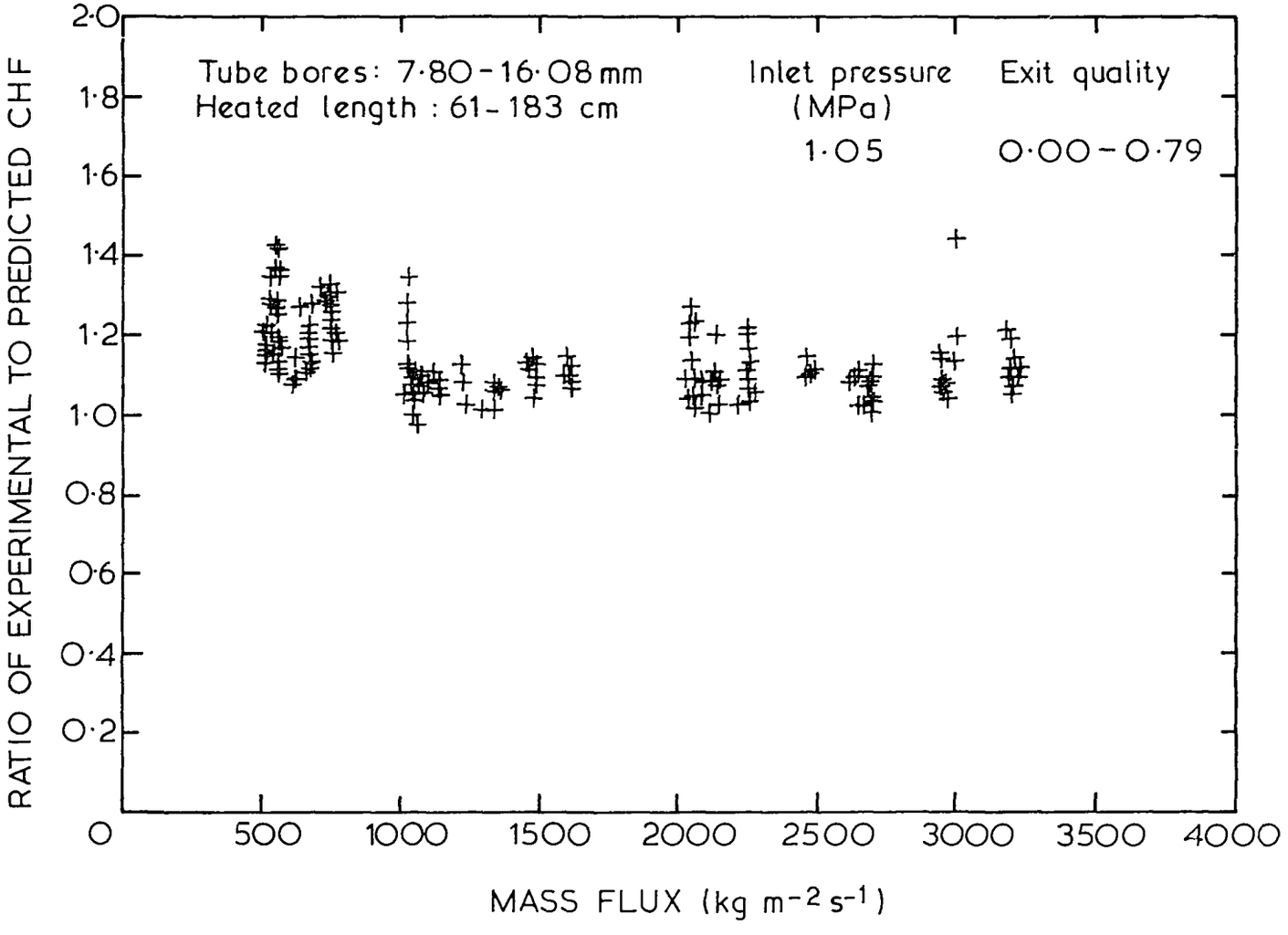

FIGURE 16. RATIO OF EXPERIMENTAL TO PREDICTED CHFs VERSUS MASS FLUX AT THE EXIT OF A UNIFORMLY HEATED TUBE USING THE BERTOLETTI CORRELATION (GROENEVELD DATA)

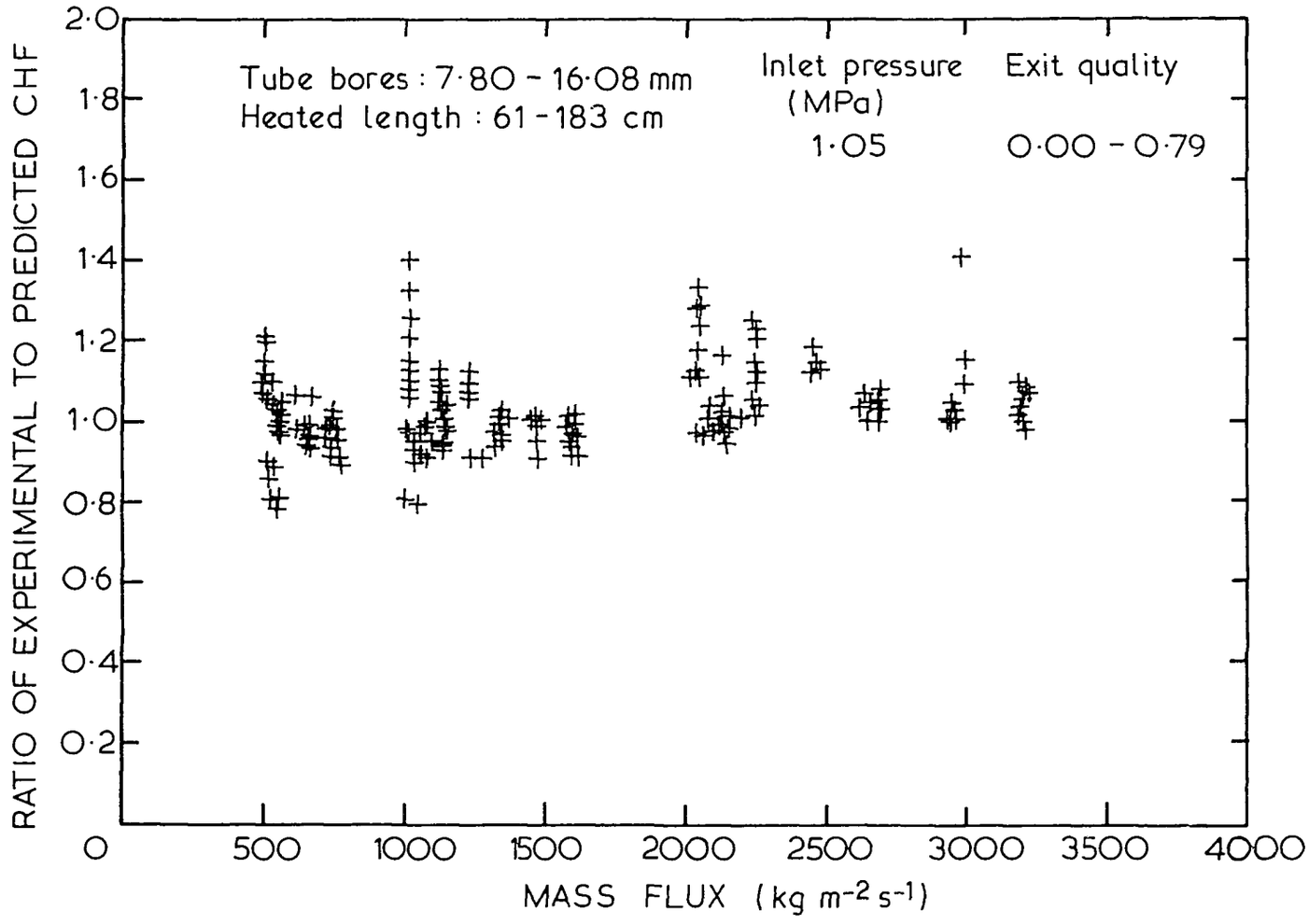

FIGURE 17. RATIO OF EXPERIMENTAL TO PREDICTED CHFs VERSUS MASS FLUX AT THE EXIT OF A UNIFORMLY HEATED TUBE USING THE MODIFIED BERTOLETTI CORRELATION (GROENEVELD DATA)

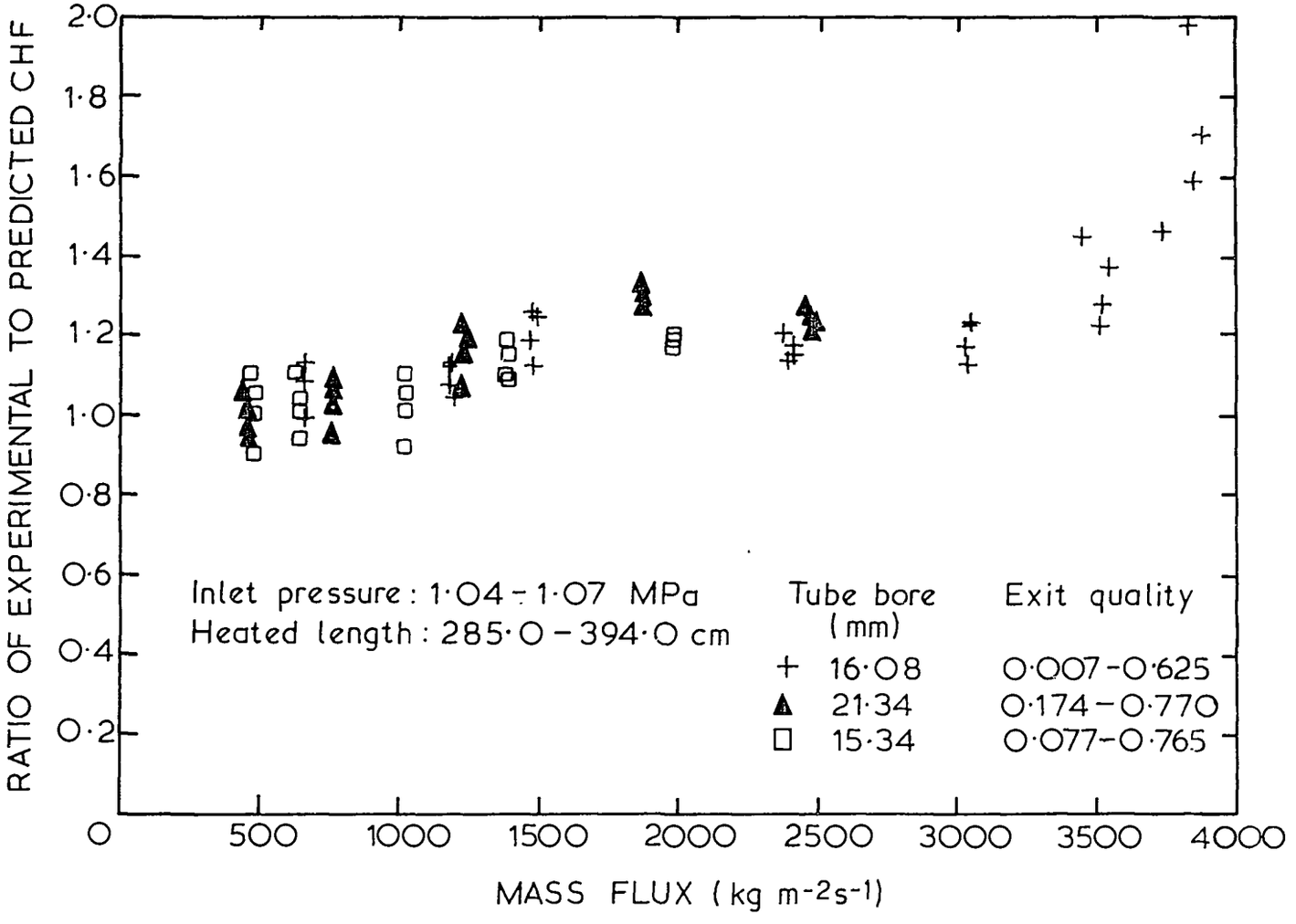

FIGURE 18. COMPARISON OF EXPERIMENTAL CHFs WITH VALUES PREDICTED BY THE MODIFIED GROENEVELD CORRELATION (STEVENS & MILES DATA)

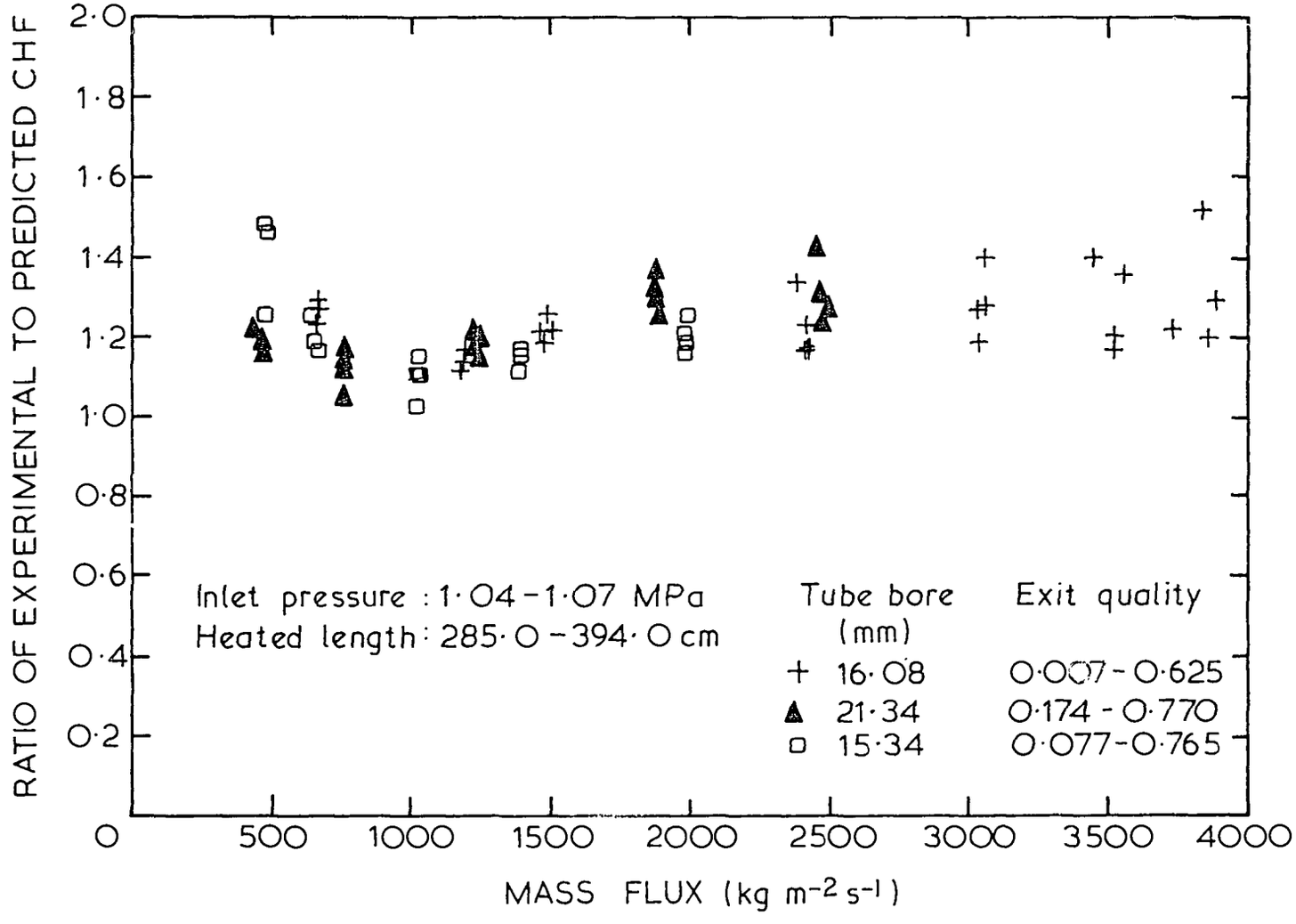

FIGURE 19. COMPARISON OF EXPERIMENTAL CHFs WITH VALUES PREDICTED BY THE BERTOLETTI CORRELATION (STEVENS & MILES DATA)

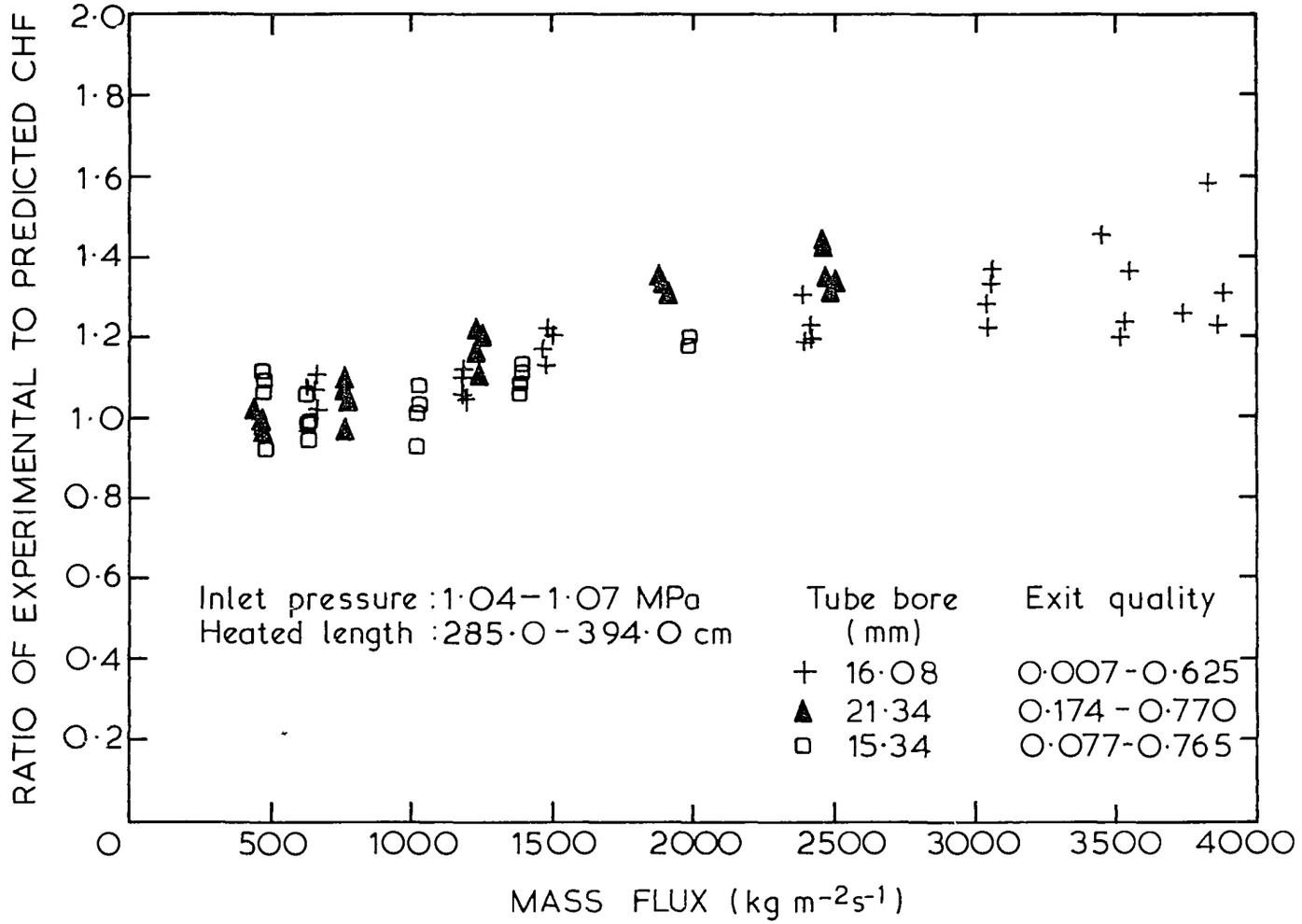

FIGURE 20. COMPARISON OF EXPERIMENTAL CHFs WITH VALUES PREDICTED BY THE MODIFIED BERTOLETTI CORRELATION (STEVENS & MILES DATA)

APPENDIX A(a)
UNIFORMLY HEATED TUBE BURNOUT DATA (TUBE 1)

Tube bore = 8.48 mm

Other tube dimensions: Wall thickness = 1.22 mm
Heated length = 2870 mm

Date	Run No.	Inlet Pressure (MPa)	Power (kW)	Pressure Drop (kPa)	Exit Quality	Mass Flux ($Mg\ s^{-1}\ m^{-2}$)	Inlet Subcooling ($kJ\ kg^{-1}$)	Heat Flux ($kW\ m^{-2}$)
	30	0.936	9.83	121.12	0.323	2.735	20.43	128.51
	33	0.937	8.54	136.51	0.340	2.790	8.59	111.64
	36	0.930	8.19	146.14	0.379	2.785	1.05	107.13
8.11.79	39	0.934	9.26	108.66	0.357	2.414	20.34	121.06
	42	0.933	8.59	116.51	0.376	2.472	11.28	112.37
	45	0.933	7.63	124.68	0.398	2.461	1.56	99.76
	48	0.932	8.13	91.07	0.372	2.036	21.33	106.37
	51	0.932	7.54	97.87	0.408	2.058	10.61	98.63
	54	0.932	6.65	101.85	0.410	2.090	1.70	86.95
	60	1.087	9.59	97.63	0.272	2.710	27.80	125.48
9.11.79	64	1.090	8.54	110.52	0.318	2.765	13.70	111.65
	68	1.089	7.41	123.92	0.367	2.772	-0.01	96.93
	72	1.091	8.94	86.12	0.303	2.351	28.52	116.91
	76	1.090	8.05	96.79	0.356	2.443	12.68	105.26
	80	1.089	6.70	105.39	0.379	2.448	-0.26	87.67
	1	1.089	8.10	77.32	0.336	2.025	27.83	105.93
	5	1.089	7.63	80.67	0.383	2.071	16.33	99.84
	9	1.090	6.33	84.13	0.405	2.063	2.49	82.79
20.11.79	13	1.094	7.54	67.06	0.391	1.720	27.81	98.60
	17	1.089	6.69	68.11	0.405	1.724	17.05	87.54
	21	1.089	5.68	67.16	0.436	1.679	4.41	74.34
	1	1.324	9.43	77.40	0.192	2.724	37.97	123.31
	5	1.325	8.39	85.99	0.245	2.713	24.93	109.79
	9	1.324	6.79	108.82	0.339	2.776	1.81	88.75
	13	1.322	9.20	75.94	0.245	2.426	37.40	120.29
	17	1.324	7.86	83.69	0.294	2.459	20.82	102.82
21.11.79	21	1.324	6.20	92.48	0.364	2.427	0.87	81.10
	25	1.323	8.51	68.61	0.307	2.017	37.57	111.36
	29	1.325	7.47	71.23	0.337	2.095	22.30	96.70
	33	1.324	6.08	74.68	0.382	2.084	5.31	79.56
	37	1.324	7.66	59.19	0.369	1.646	37.73	100.21
	41	1.324	6.48	60.24	0.394	1.697	19.96	84.81
22.11.79	45	1.323	5.29	59.81	0.412	1.695	5.38	69.16

APPENDIX A(b)

UNIFORMLY HEATED TUBE BURNOUT DATA (TUBE 2)

Tube bore = 16.76 mm

Other tube dimensions: Wall thickness = 1.22 mm
Heated length = 2870 mm

Date	Run No.	Inlet Pressure (MPa)	Power (kW)	Pressure Drop (kPa)	Exit Quality	Mass Flux ($Mg\ s^{-1}\ m^{-2}$)	Inlet Subcooling ($kJ\ kg^{-1}$)	Heat Flux ($kW\ m^{-2}$)
5.12.79	1	0.931	14.47	27.48	0.583	0.666	22.24	95.75
	5	0.928	13.49	26.33	0.575	0.682	14.35	89.30
	9	0.930	12.45	23.91	0.624	0.684	0.89	82.37
	13	0.928	14.20	26.01	0.635	0.611	22.24	93.99
	17	0.926	13.11	24.75	0.627	0.616	14.34	86.75
	21	0.926	12.30	22.66	0.668	0.613	3.38	81.37
6.12.79	30	0.935	13.93	23.68	0.733	0.527	23.99	92.19
	34	0.923	12.94	22.22	0.736	0.529	14.44	85.60
	38	0.925	11.80	20.02	0.750	0.527	3.28	78.08
	42	0.925	12.18	20.55	0.827	0.422	22.59	80.60
	46	0.925	11.62	19.08	0.839	0.428	13.30	76.89
	50	0.925	10.69	17.09	0.856	0.422	2.70	70.72
10.3.80	70	0.918	15.75	31.34	0.467	0.906	17.35	104.22
	74	0.919	15.32	30.40	0.490	0.912	11.81	101.39
	78	0.919	12.93	27.99	0.510	0.871	0.30	85.56
19.12.79	60	1.082	15.16	27.98	0.537	0.701	29.97	100.32
	64	1.083	13.92	25.46	0.564	0.702	18.49	92.09
	68	1.083	12.25	23.16	0.577	0.703	6.00	81.04
20.12.79	1	1.080	14.48	26.09	0.587	0.626	30.55	95.85
	5	1.080	12.96	23.16	0.614	0.626	16.08	85.76
	9	1.080	11.67	20.96	0.637	0.619	4.90	77.24
	13	1.080	13.73	23.68	0.705	0.523	29.69	90.84
11.1.80	1	1.080	12.77	21.39	0.707	0.549	15.99	84.49
	5	1.078	11.10	18.98	0.709	0.547	2.35	73.46
	9	1.079	12.29	21.39	0.784	0.432	29.92	81.35
	13	1.080	11.53	18.98	0.823	0.438	15.37	76.32
	17	1.080	9.98	16.66	0.808	0.436	1.71	66.03

(Continued)

Date	Run No.	Inlet Pressure (MPa)	Power (kW)	Pressure Drop (kPa)	Exit Quality	Mass Flux ($Mg\ s^{-1}\ m^{-2}$)	Inlet Subcooling ($kJ\ kg^{-1}$)	Heat Flux ($kW\ m^{-2}$)
5.3.80	52	1.086	16.09	30.66	0.435	0.889	26.96	106.50
	56	1.085	14.56	28.88	0.457	0.907	14.93	96.35
	60	1.086	12.88	26.99	0.471	0.892	5.87	85.24
16.1.80	10	1.316	11.21	21.61	0.554	0.701	5.82	74.18
	14	1.316	14.51	27.38	0.536	0.633	39.31	96.00
	18	1.316	12.75	24.34	0.581	0.623	22.91	84.35
	22	1.317	10.57	19.61	0.609	0.633	2.45	69.93
	26	1.315	13.63	25.50	0.619	0.543	39.26	90.20
	30	1.317	12.17	22.35	0.665	0.536	22.97	80.51
17.1.80	1	1.316	10.29	18.45	0.671	0.544	5.11	68.09
	5	1.317	12.11	23.18	0.735	0.432	38.69	80.12
	9	1.318	11.13	20.56	0.744	0.440	25.11	73.62
	13	1.317	9.23	16.25	0.745	0.455	2.58	61.06
5.3.80	40	1.312	16.19	31.60	0.380	0.896	36.07	107.13
	44	1.314	14.59	28.77	0.432	0.891	22.15	96.57
	48	1.315	11.52	24.29	0.448	0.896	4.37	76.23

APPENDIX A(c)
UNIFORMLY HEATED TUBE BURNOUT DATA (TUBE 3)

Tube bore = 21.34 mm

Other tube dimensions: Wall thickness = 2.03 mm
Heated length = 3700 mm

Date	Run No.	Inlet Pressure (MPa)	Power (kW)	Pressure Drop (kPa)	Exit Quality	Mass Flux ($Mg\ s^{-1}\ m^{-2}$)	Inlet Subcooling ($kJ\ kg^{-1}$)	Heat Flux ($kW\ m^{-2}$)
10.4.79	98	0.918	17.71	23.11	0.763	0.412	24.05	71.38
27.3.79	33	0.917	16.65	21.41	0.772	0.422	12.24	67.11
	41	0.916	15.69	18.18	0.788	0.434	1.85	63.25
28.3.79	44	0.916	20.42	28.04	0.540	0.703	13.62	82.31
	47	0.916	17.92	24.06	0.561	0.682	2.21	72.80
29.3.79	51	0.914	24.23	35.42	0.401	1.031	15.16	97.67
	54	0.916	20.45	31.34	0.429	1.012	1.59	82.43
11.4.79	101	0.929	26.43	38.01	0.357	1.048	25.36	106.56
	104	0.930	22.71	30.04	0.538	0.684	24.83	91.56
	1	0.921	17.73	21.80	0.819	0.383	23.41	71.48
	4	0.921	16.89	19.29	0.839	0.387	13.76	68.08
	7	0.922	15.43	16.67	0.839	0.389	2.94	62.19
	10	0.921	21.91	28.18	0.565	0.639	23.09	88.33
24.10.79	13	0.921	20.19	26.09	0.577	0.644	13.70	81.38
	16	0.922	18.88	22.96	0.616	0.639	3.86	76.11
	19	0.926	26.96	36.04	0.423	0.965	24.58	108.69
	22	0.922	24.07	33.11	0.432	0.961	14.27	97.06
	25	0.922	21.04	29.34	0.464	0.968	1.23	84.83
	14	1.089	17.26	24.18	0.727	0.402	31.00	69.58
21.3.79	17	1.089	15.71	21.25	0.752	0.410	16.31	63.34
	20	1.089	13.93	17.57	0.771	0.405	2.93	56.16
	2	1.087	21.72	31.54	0.517	0.669	29.98	87.54
6.3.79	5	1.089	19.70	27.73	0.532	0.670	17.78	79.43
	8	1.089	17.74	23.50	0.565	0.679	3.31	71.51
	2	1.087	27.07	38.84	0.361	1.030	30.83	109.14
8.3.79	5	1.087	23.13	34.40	0.390	1.029	15.89	93.35
	8	1.089	20.37	30.38	0.423	1.028	3.66	82.12
	28	1.094	18.23	22.75	0.816	0.388	31.43	73.48
24.10.79	31	1.095	16.01	19.60	0.818	0.387	15.94	64.54
	34	1.095	14.82	16.05	0.846	0.386	3.47	59.75

Date	Run No.	Inlet Pressure (MPa)	Power (kW)	Pressure Drop (kPa)	Exit Quality	Mass Flux ($Mg\ s^{-1}\ m^{-2}$)	Inlet Subcooling ($kJ\ kg^{-1}$)	Heat Flux ($kW\ m^{-2}$)
	40	1.090	22.53	29.02	0.558	0.627	31.29	90.83
	43	1.094	19.52	26.09	0.549	0.641	17.33	78.70
	46	1.094	18.08	21.80	0.619	0.631	4.19	72.87
25.10.79	49	1.090	27.60	36.34	0.388	0.966	32.04	111.28
	52	1.095	23.53	32.58	0.416	0.968	16.84	94.85
	55	1.095	19.99	28.92	0.434	0.963	4.47	80.57
	60	1.323	17.84	25.57	0.749	0.389	40.42	71.92
	63	1.323	16.36	21.49	0.829	0.384	22.91	65.95
	66	1.322	14.29	16.88	0.813	0.400	5.16	57.62
29.3.79	57	1.318	23.62	35.64	0.353	1.032	23.74	95.20
	60	1.318	18.22	30.08	0.379	1.041	5.53	73.46
	66	1.326	19.08	29.73	0.469	0.692	24.65	76.90
	69	1.326	15.61	23.76	0.520	0.672	5.68	62.91
30.3.79	72	1.326	15.68	23.03	0.757	0.397	24.36	63.20
	75	1.328	13.55	18.73	0.749	0.411	6.58	54.64
	85	1.326	27.63	39.94	0.307	1.035	41.00	111.40
10.4.79	88	1.326	21.62	33.56	0.426	0.688	40.40	87.15
	91	1.326	17.46	26.77	0.675	0.416	40.60	70.39
26.10.79	1	1.316	18.48	25.36	0.791	0.382	40.16	74.48
	6	1.320	22.34	32.16	0.4[illegible]	0.631	39.70	90.07
	10	1.321	20.21	28.61	0.5[illegible]	0.632	25.45	81.48
	14	1.321	16.92	22.75	0.567	0.634	6.45	68.20
	18	1.320	27.48	38.44	0.331	0.962	39.93	110.80
	22	1.319	23.51	34.67	0.366	0.964	24.04	94.78
	26	1.322	18.43	28.40	0.422	0.934	4.44	74.31

APPENDIX B(a)

NON-UNIFORMLY HEATED TUBE BURNOUT DATA FROM STEP 3 (TUBE 1)

Tube bore = 8.48 mm

Other tube dimensions: Wall thickness = 1.22 mm
Heated length of Section 1 = 2870 mm
Heated length of Section 2 = 230 mm

Date	Run No.	Inlet Pressure (MPa)	Power (kW)	Pressure Drop (kPa)	Exit Quality	Mass Flux ($Mg\ s^{-1}\ m^{-2}$)	Inlet Subcooling ($kJ\ kg^{-1}$)	Surface Heat Fluxes Section 1 ($kW\ m^{-2}$)	Section 2 ($kW\ m^{-2}$)
	31	0.932	9.38	126.45	0.333	2.728	19.69	122.74	84.46
	34	0.933	8.30	139.97	0.357	2.769	8.22	108.54	77.66
	37	0.933	7.59	148.97	0.373	2.780	1.03	99.30	74.25
8.11.79	40	0.932	8.42	112.01	0.347	2.403	20.24	110.16	98.64
	43	0.930	8.32	120.07	0.390	2.456	10.97	108.80	72.48
	46	0.934	7.24	126.98	0.399	2.455	1.51	94.66	62.27
	49	0.933	8.04	94.20	0.392	2.032	21.45	105.19	63.76
9.11.79	52	0.933	7.04	99.23	0.401	2.063	10.61	92.01	67.20
	55	0.933	6.40	105.62	0.424	2.083	1.57	83.71	70.25

APPENDIX B(b)

NON-UNIFORMLY HEATED TUBE BURNOUT DATA FROM STEP 3 (TUBE 3)

Tube bore = 21.34 mm

Other tube dimensions: Wall thickness = 2.03 mm
Heated length of Section 1 = 3700 mm
Heated length of Section 2 = 230 mm

Date	Run No.	Inlet Pressure (MPa)	Power (kW)	Pressure Drop (kPa)	Exit Quality	Mass Flux ($Mg\ s^{-1}\ m^{-2}$)	Inlet Subcooling ($kJ\ kg^{-1}$)	Surface Heat Fluxes Section 1 ($kW\ m^{-2}$)	Section 2 ($kW\ m^{-2}$)
	2	0.921	16.95	22.53	0.828	0.382	23.57	68.34	72.83
	5	0.922	15.52	20.13	0.803	0.388	13.59	62.58	62.61
	8	0.922	14.49	17.31	0.821	0.389	2.91	58.42	56.77
	11	0.922	20.99	29.13	0.556	0.638	23.30	84.64	64.02
	14	0.922	19.75	26.30	0.577	0.644	13.76	79.61	55.35
24.10.79	17	0.922	17.88	23.69	0.599	0.641	4.03	72.10	67.09
	20	0.924	25.83	36.77	0.410	0.963	24.62	104.13	78.15
	23	0.922	22.72	33.94	0.421	0.961	14.23	91.59	76.92
	26	0.922	20.04	29.96	0.451	0.966	1.20	80.79	54.55
	29	1.095	17.06	23.90	0.766	0.389	31.44	68.76	50.02
	32	1.095	15.26	20.13	0.801	0.389	15.31	61.51	60.18
	35	1.095	13.79	16.57	0.810	0.388	2.82	55.61	49.54
	41	1.095	21.99	30.17	0.560	0.626	31.46	88.66	57.73
	44	1.094	19.27	26.83	0.570	0.641	17.10	77.69	75.56
	47	1.094	16.74	22.64	0.595	0.628	4.16	67.48	68.99
	50	1.094	26.32	37.92	0.380	0.963	32.13	106.10	85.10
25.10.79	53	1.095	22.07	33.52	0.400	0.968	16.80	88.98	80.84
	56	1.096	19.71	29.02	0.443	0.964	3.78	79.45	57.96
	61	1.323	16.43	26.72	0.719	0.388	40.38	66.25	75.61
	64	1.322	15.03	22.32	0.771	0.390	22.63	60.61	66.43
	67	1.322	12.93	17.61	0.781	0.392	4.70	52.11	58.11

APPENDIX C(a)

NON-UNIFORMLY HEATED TUBE BURNOUT DATA FROM STEP 3A (TUBE 1)

Tube bore = 8.48 mm

Other tube dimensions: Wall thickness = 1.22 mm

Heated length of Section 1 = 2870 mm

Heated length of Section 2 = 230 mm

Date	Run No.	Inlet Pressure (MPa)	Power (kW)	Pressure Drop (kPa)	Exit Quality	Mass Flux ($Mg\ s^{-1}\ m^{-2}$)	Inlet Subcooling ($kJ\ kg^{-1}$)	Surface Heat Fluxes Section 1 ($kW\ m^{-2}$)	Section 2 ($kW\ m^{-2}$)
	61	1.091	9.42	97.84	0.275	2.710	27.96	123.23	42.62
	65	1.093	8.69	110.62	0.344	2.776	13.81	113.64	68.24
9.11.79	69	1.091	7.54	123.40	0.377	2.783	0.13	98.63	20.78
	73	1.082	8.83	86.54	0.302	2.352	28.32	115.47	13.01
	77	1.090	7.90	98.68	0.375	2.432	12.39	103.28	68.73
	81	1.091	6.69	106.22	0.387	2.446	-0.18	87.54	24.07
	2	1.087	8.25	77.01	0.348	2.037	27.78	107.94	8.80
	6	1.089	7.39	81.51	0.374	2.071	16.29	96.60	18.34
20.11.79	10	1.090	6.06	84.96	0.394	2.070	2.45	79.20	21.24
	14	1.087	7.57	67.68	0.408	1.714	27.30	99.01	18.70
	18	1.090	6.67	68.42	0.414	1.724	17.09	87.28	20.78
	22	1.093	5.52	67.68	0.432	1.673	4.55	72.16	18.34
	2	1.324	9.12	77.40	0.187	2.713	38.17	119.34	32.34
	6	1.323	8.69	85.47	0.277	2.696	24.65	113.67	32.32
	10	1.324	6.62	107.25	0.342	2.780	1.87	86.62	38.05
	14	1.325	9.03	76.15	0.252	2.420	37.54	118.12	46.04
	18	1.324	7.98	83.27	0.307	2.474	20.63	104.42	20.13
21.11.79	22	1.325	5.97	91.54	0.358	2.427	0.73	78.08	16.79
	26	1.325	8.64	67.45	0.328	2.015	37.71	113.07	28.17
	30	1.325	7.45	71.23	0.350	2.072	22.30	97.50	18.53
	34	1.325	5.90	74.79	0.373	2.090	5.36	77.15	11.28
	38	1.324	7.75	59.29	0.388	1.652	37.73	101.33	24.70
	42	1.324	6.45	60.24	0.397	1.697	19.96	84.42	9.63
	46	1.324	5.27	60.76	0.426	1.683	5.17	68.98	19.88

APPENDIX C(b)

NON-UNIFORMLY HEATED TUBE BURNOUT DATA FROM STEP 3A (TUBE 2)

Tube bore = 16.76 mm

Other tube dimensions: Wall thickness = 1.22 mm
Heated length of Section 1 = 2870 mm
Heated length of Section 2 = 230 mm

Date	Run No.	Inlet Pressure (MPa)	Power (kW)	Pressure Drop (kPa)	Exit Quality	Mass Flux ($Mg\ s^{-1}\ m^{-2}$)	Inlet Subcooling ($kJ\ kg^{-1}$)	Surface Heat Fluxes Section 1 ($kW\ m^{-2}$)	Section 2 ($kW\ m^{-2}$)
10.3.79	71	0.919	15.62	31.13	0.466	0.905	17.43	103.35	7.36
	75	0.919	15.20	30.40	0.487	0.912	12.01	100.61	7.44
	79	0.919	12.91	27.88	0.509	0.875	0.51	85.43	6.52
5.12.79	2	0.930	14.36	27.48	0.583	0.665	22.18	95.03	8.12
	6	0.928	13.48	26.33	0.578	0.682	14.35	89.23	7.00
	10	0.927	12.44	24.12	0.628	0.684	0.76	82.31	7.63
	14	0.927	14.04	26.01	0.628	0.614	22.18	92.93	8.55
	18	0.926	13.05	24.55	0.634	0.612	14.35	86.38	7.63
	22	0.926	12.17	22.45	0.665	0.615	3.18	80.51	5.80
6.12.79	31	0.928	13.98	23.37	0.741	0.529	23.71	92.53	7.28
	35	0.922	13.13	22.01	0.750	0.530	14.38	86.86	5.43
	39	0.923	11.49	20.02	0.735	0.527	3.22	76.01	6.14
	43	0.923	12.11	20.55	0.835	0.419	22.53	80.16	6.58
	47	0.925	11.70	19.08	0.852	0.428	13.30	77.45	5.96
	51	0.925	10.78	17.19	0.868	0.424	2.69	71.33	7.28
19.12.79	61	1.083	15.34	27.87	0.554	0.700	30.03	101.48	11.14
	65	1.082	14.06	25.56	0.577	0.701	18.43	93.07	6.72
	69	1.083	12.28	22.95	0.584	0.701	6.01	81.24	6.90
20.12.79	2	1.080	14.57	26.20	0.600	0.626	30.55	96.40	10.68
	6	1.080	12.85	23.27	0.611	0.627	16.08	85.01	7.09
	10	1.082	12.03	20.85	0.663	0.618	5.17	79.60	7.68
	14	1.080	13.65	23.68	0.705	0.523	29.69	90.30	6.56
10.1.80	2	1.080	12.48	21.39	0.697	0.547	15.69	82.60	5.50
11.1.80	6	1.080	11.19	18.80	0.723	0.544	2.68	74.07	8.11
	10	1.080	12.28	21.39	0.791	0.432	29.97	81.29	8.01
	14	1.080	11.38	18.98	0.824	0.434	15.37	75.33	5.79
	18	1.082	9.90	16.77	0.807	0.436	1.76	65.50	5.72

(Continued)

Date	Run No.	Inlet Pressure (MPa)	Power (kW)	Pressure Drop (kPa)	Exit Quality	Mass Flux ($Mg\ s^{-1}\ m^{-2}$)	Inlet Subcooling ($kJ\ kg^{-1}$)	Surface Heat Fluxes Section 1 ($kW\ m^{-2}$)	Section 2 ($kW\ m^{-2}$)
5.3.80	53	1.087	15.70	30.66	0.424	0.889	27.01	103.88	10.59
	57	1.086	14.49	28.77	0.459	0.905	14.99	95.92	7.58
	61	1.087	13.14	26.58	0.485	0.890	5.94	86.99	5.12
16.1.80	11	1.316	11.38	21.71	0.570	0.701	5.71	75.30	8.41
	15	1.317	14.87	27.38	0.565	0.635	39.35	98.42	12.34
	19	1.317	12.83	24.03	0.592	0.624	22.68	84.88	7.89
	23	1.317	10.70	19.51	0.627	0.632	2.11	70.78	8.95
	27	1.320	13.46	25.60	0.623	0.540	39.44	89.06	14.84
	31	1.318	11.92	22.35	0.655	0.536	23.02	78.89	8.90
17.2.80	2	1.317	10.48	18.45	0.692	0.543	5.15	69.35	7.24
	6	1.320	12.20	23.08	0.747	0.435	38.79	80.70	11.41
	10	1.318	11.06	20.66	0.749	0.440	25.10	73.20	9.82
	14	1.318	9.52	16.36	0.776	0.455	2.62	63.00	7.72
5.3.80	41	1.314	16.12	31.08	0.385	0.897	36.13	106.68	17.29
	45	1.315	14.41	28.57	0.430	0.891	22.21	95.38	10.68
	49	1.314	11.85	24.59	0.471	0.897	3.89	78.45	10.42

APPENDIX C(c)

NON-UNIFORMLY HEATED TUBE BURNOUT DATA FROM STEP 3A (TUBE 3)

Tube bore = 21.34 mm

Other tube dimensions: Wall thickness = 2.03 mm
Heated length of Section 1 = 2870 mm
Heated length of Section 2 = 230 mm

Date	Run No.	Inlet Pressure (MPa)	Power (kW)	Pressure Drop (kPa)	Exit Quality	Mass Flux ($Mg\ s^{-1}\ m^{-2}$)	Inlet Subcooling ($kJ\ kg^{-1}$)	Surface Heat Fluxes Section 1 ($kW\ m^{-2}$)	Section 2 ($kW\ m^{-2}$)
26.10.79	2	1.320	17.30	26.09	0.731	0.386	40.27	69.75	24.80
	7	1.321	22.31	32.16	0.510	0.632	39.75	89.94	35.52
	11	1.321	19.47	28.92	0.517	0.637	25.43	78.48	33.37
	15	1.321	16.80	22.43	0.608	0.607	6.03	67.74	22.44
	19	1.322	27.33	38.76	0.342	0.961	40.01	110.18	37.32
	23	1.326	23.24	34.37	0.365	0.968	24.33	93.69	23.70
	27	1.324	18.88	28.29	0.444	0.927	4.28	76.11	16.28

APPENDIX D(a)

NON-UNIFORMLY HEATED TUBE BURNOUT DATA FROM STEP 3B (TUBE 1)

Tube bore = 8.48 mm

Other tube dimensions: Wall thickness = 1.22 mm
Heated length of Section 1 = 2870 mm
Heated length of Section 2 = 230 mm

Date	Run No.	Inlet Pressure (MPa)	Power (kW)	Pressure Drop (kPa)	Exit Quality	Mass Flux ($Mg\ s^{-1}\ m^{-2}$)	Inlet Subcooling ($kJ\ kg^{-1}$)	Surface Heat Fluxes Section 1 ($kW\ m^{-2}$)	Surface Heat Fluxes Section 2 ($kW\ m^{-2}$)
	62	1.089	9.45	101.61	0.298	2.697	27.68	123.57	97.79
	66	1.089	7.99	114.91	0.322	2.760	13.45	104.47	94.79
9.11.79	70	1.090	7.20	127.58	0.386	2.768	-0.12	94.23	92.01
	74	1.091	8.58	89.15	0.306	2.341	28.60	112.23	63.08
	78	1.090	7.65	100.77	0.371	2.421	12.29	100.11	88.91
	82	1.089	6.44	106.85	0.385	2.442	-0.32	84.23	56.25
	3	1.087	7.72	79.72	0.353	2.031	27.39	100.92	97.99
	7	1.089	7.32	82.66	0.385	2.065	16.24	95.76	53.10
20.11.79	11	1.089	5.99	86.95	0.418	2.058	2.10	78.37	76.82
	15	1.090	7.14	69.47	0.403	1.714	27.54	93.37	81.87
	19	1.090	6.38	69.88	0.406	1.723	17.03	83.39	52.52
	23	1.093	5.19	70.09	0.419	1.679	4.24	67.88	44.05
	3	1.323	9.00	80.54	0.209	2.703	38.01	117.67	110.15
	7	1.323	8.53	89.55	0.293	2.678	24.20	111.58	85.66
	11	1.324	6.51	109.97	0.350	2.769	1.77	85.19	74.09
	15	1.324	8.96	78.14	0.273	2.432	37.41	117.19	118.67
	19	1.324	8.02	85.78	0.335	2.457	20.54	104.90	78.40
21.11.79	23	1.325	5.88	93.85	0.369	2.427	0.43	76.97	54.91
	27	1.325	8.50	69.76	0.341	2.026	37.62	111.13	87.34
	31	1.325	7.46	73.63	0.367	2.072	22.21	97.56	57.81
	35	1.324	5.81	75.73	0.385	2.077	5.27	75.93	49.16
	39	1.325	7.35	60.65	0.375	1.663	37.93	96.16	77.09
	43	1.325	6.07	61.59	0.396	1.691	19.96	79.44	66.39
22.11.79	47	1.324	5.09	60.97	0.420	1.683	5.17	66.60	37.69

APPENDIX D(b)

NON-UNIFORMLY HEATED TUBE BURNOUT DATA FROM STEP 3B (TUBE 2)

Tube bore = 16.76 mm

Other tube dimensions: Wall thickness = 1.22 mm
Heated length of Section 1 = 2870 mm
Heated length of Section 2 = 230 mm

Date	Run No.	Inlet Pressure (MPa)	Power (kW)	Pressure Drop (kPa)	Exit Quality	Mass Flux ($Mg\ s^{-1}\ m^{-2}$)	Inlet Subcooling ($kJ\ kg^{-1}$)	Surface Heat Fluxes Section 1 ($kW\ m^{-2}$)	Section 2 ($kW\ m^{-2}$)
	3	0.930	14.14	28.32	0.604	0.665	22.14	93.60	58.64
	7	0.928	12.95	27.27	0.586	0.678	14.31	85.67	56.38
5.12.79	11	0.926	11.39	24.65	0.594	0.684	0.68	75.38	37.67
	15	0.926	13.87	26.95	0.649	0.613	21.79	91.78	47.91
	19	0.927	12.70	25.28	0.636	0.613	13.87	84.07	36.11
	23	0.927	11.80	23.18	0.672	0.616	3.00	78.09	46.15
	32	0.922	13.53	23.89	0.739	0.525	23.38	89.51	33.35
	36	0.923	12.44	22.43	0.741	0.532	14.22	82.35	50.97
6.12.79	40	0.923	10.93	20.64	0.730	0.527	3.19	72.30	46.05
	44	0.925	11.75	21.17	0.835	0.420	22.56	77.74	38.90
	48	0.925	11.21	19.70	0.850	0.428	13.27	74.21	44.66
	52	0.925	10.14	17.92	0.855	0.425	2.66	67.10	49.94
	72	0.919	15.08	32.48	0.480	0.904	17.36	99.78	79.25
10.3.80	76	0.919	14.27	31.75	0.493	0.912	11.66	94.45	91.84
	80	0.920	12.25	29.03	0.519	0.876	0.21	81.06	78.78
	62	1.082	14.29	28.71	0.535	0.698	29.94	94.56	63.19
19.12.79	66	1.082	13.13	26.61	0.571	0.700	18.39	86.91	70.64
	70	1.083	11.82	24.00	0.591	0.700	5.96	78.20	53.70
	3	1.080	14.57	26.51	0.626	0.626	30.54	96.45	48.64
20.12.79	7	1.080	12.04	24.42	0.606	0.627	15.82	79.64	63.33
	11	1.082	11.30	21.69	0.654	0.617	5.14	74.76	54.96
	15	1.080	12.75	24.73	0.705	0.521	29.65	84.38	73.93
10.1.80	3	1.080	12.09	22.35	0.712	0.548	15.65	80.02	57.48
	7	1.079	10.35	19.71	0.707	0.544	2.59	68.46	57.16
11.1.80	11	1.080	11.79	22.14	0.796	0.432	29.94	77.99	53.84
	15	1.080	10.94	19.71	0.832	0.436	15.14	72.40	52.35
	19	1.080	9.74	17.19	0.837	0.434	1.68	64.47	45.27

(Continued)

Date	Run No.	Inlet Pressure (MPa)	Power (kW)	Pressure Drop (kPa)	Exit Quality	Mass Flux ($Mg\ s^{-1}\ m^{-2}$)	Inlet Subcooling ($kJ\ kg^{-1}$)	Surface Heat Fluxes Section 1 ($kW\ m^{-2}$)	Surface Heat Fluxes Section 2 ($kW\ m^{-2}$)
	54	1.086	15.82	31.50	0.457	0.888	26.92	104.68	63.64
5.3.80	58	1.086	14.03	29.93	0.476	0.903	15.14	92.84	80.96
	62	1.087	12.20	27.83	0.482	0.889	5.89	80.72	74.66
	12	1.316	10.57	22.45	0.552	0.701	5.68	69.94	48.03
	16	1.316	14.32	28.12	0.573	0.632	39.28	94.76	64.13
16.1.80	20	1.316	11.94	25.18	0.586	0.623	22.59	79.00	71.10
	24	1.317	9.84	20.66	0.617	0.633	2.07	65.09	65.96
	28	1.317	12.16	27.08	0.596	0.540	39.49	80.46	90.13
	32	1.317	11.16	23.08	0.634	0.539	22.54	73.83	47.38
	3	1.316	9.34	19.30	0.648	0.544	4.75	61.78	48.42
17.1.80	7	1.318	11.90	23.50	0.761	0.433	38.73	78.76	44.72
	11	1.317	10.10	21.71	0.733	0.437	25.02	66.86	66.45
	15	1.318	8.81	17.09	0.762	0.453	2.60	58.28	49.26
	42	1.314	15.69	32.02	0.405	0.896	35.83	103.86	85.78
5.3.80	46	1.314	13.46	29.62	0.422	0.890	22.12	89.08	70.35
	50	1.315	11.00	25.32	0.469	0.897	3.70	72.82	73.22

APPENDIX D(c)
NON-UNIFORMLY HEATED TUBE BURNOUT DATA FROM STEP 3B (TUBE 3)

Tube bore = 21.34 mm

Other tube dimensions: Wall thickness = 2.03 mm
Heated length of Section 1 = 3700 mm
Heated length of Section 2 = 230 mm

Date	Run No.	Inlet Pressure (MPa)	Power (kW)	Pressure Drop (kPa)	Exit Quality	Mass Flux ($Mg\ s^{-1}\ m^{-2}$)	Inlet Subcooling ($kJ\ kg^{-1}$)	Surface Heat Fluxes Section 1 ($kW\ m^{-2}$)	Section 2 ($kW\ m^{-2}$)
26.10.79	3	1.321	16.39	27.24	0.761	0.379	40.28	66.09	94.61
	8	1.321	21.22	33.11	0.490	0.640	39.91	85.54	92.44
	12	1.321	19.01	29.66	0.527	0.636	25.61	76.63	81.48
	16	1.321	16.06	22.96	0.566	0.638	6.01	64.74	53.43
	20	1.322	25.93	39.17	0.327	0.959	40.19	104.53	90.06
	24	1.321	21.90	35.61	0.373	0.936	24.30	88.30	83.20
	28	1.324	17.91	28.81	0.439	0.922	4.26	72.19	58.41

Printed by the AAEC Research Establishment